34. Orbit and Clock Product Generation

Jan P. Weiss, Peter Steigenberger, Tim Springer

Many sophisticated Global Navigation Satellite System (GNSS) applications require high-precision satellite orbit and clock products. The GNSS orbits and clocks are usually derived from the analysis of tracking data collected by a globally distributed GNSS receiver network. The estimation process adjusts parameters for the satellite orbits, transmitter and receiver clocks, station positions, tropospheric delays, Earth orientation, intersystem and interfrequency biases, and carrier-phase ambiguities. The estimation requires detailed modeling of geophysical processes, atmospheric and relativistic effects, receiver tracking modes, antenna phase centers, spacecraft properties, and attitude control algorithms. This chapter describes precise orbit and clock determination of the GNSS constellations as performed by the analysis centers of the International GNSS Service, including models, estimation strategies, products, and the combination of orbit and clock solutions.

Most applications of GNSS rely on knowledge of the orbital positions and clock offsets of the transmitter satellites. These parameters are obtained from an estimation process that combines tracking data from terrestrial stations, measurement models, and satellite force models to adjust a set of parameters representing station positions, atmospheric delays, satellite orbits, clock offsets, and the Earth's orientation.

There are broadly three communities performing routine orbit and clock determination of the GNSS constellations: the control segments, the analysis centers (ACs) of the International GNSS Service (IGS; Chap. 33), and commercial services. The GNSS operational control segments perform orbit and clock determination in real time or near real time using tracking data from a limited set of highly secure ground stations. The orbit and clock solutions are then predicted forward and transmitted to users via the navigation message for real-time use. While the Global Positioning System (GPS) and Global'naya Navigatsionnaya Sput-

nikova Sistema (GLONASS) broadcast orbit and clock have been very good in recent years, they are nevertheless significantly less accurate than solutions produced by the IGS or comparable precise services [34.1]. The main reason for this is that the broadcast orbit and clock is predicted based on a *zero age of data* solution derived from a small tracking network. The prediction time-span can be significant: currently for GPS and GLONASS the update interval can be as long as 24 h. For Galileo, the update rate is reduced to about 100 min, which makes more accurate broadcast ephemerides possible. However, the accuracy of broadcast ephemerides is not likely to become sufficient for applications requiring decimeter or better positioning and time transfer, which in turn drives the need for more accurate and precise orbit determination (POD) and clock products.

The main goals of the IGS are to collect and archive GNSS data from a global network, and to generate precise products for the GNSS constellations. The products of the IGS, in particular the orbits, clocks, and station positions give users direct access to the International Terrestrial Reference Frame (ITRF) with accuracies not previously available with such ease. By taking at least one of the stations of the IGS tracking network, the IGS orbits, and the IGS station position solution, a user can position a network of stations with millimeter precision in the global reference frame. The high quality and public availability of the IGS products have led to the use of GNSS for many new applications, for example, meteorology and time transfer, and most certainly paved the way for commercial high-accuracy GNSS services operating in the market today. Details of the roles and products of the IGS are given in Chap. 33.

Commercial services typically aim to bridge the gap between the control segment solutions, which are very robust but have lower accuracy, and products available from the IGS, which are very accurate but provided on a *best effort* basis. These services generally cater to precise real-time navigation needs of, for example, the maritime and agricultural industries.

This chapter describes what is required for the generation of highly accurate GNSS orbit and clock products for the most demanding applications. We discuss the tracking network, describe relevant models, key GNSS system parameters, estimation strategies, and software implementations. We summarize post-processed GNSS products available from analysis and combination centers, and look at POD for multiple GNSS constellations.

34.1 Global Tracking Network

GNSS POD requires geodetic GNSS tracking stations providing at least dual-frequency measurements to account for ionospheric path delays. A globally distributed tracking station network is needed to ensure adequate observation strength for all satellites at every epoch in the processing arc. This particularly benefits clock offset determination since these parameters are normally not constrained in the estimation. Due to the unknown satellite and receiver clock offsets, and the ambiguous carrier-phase observations, GNSS phase observations contain only limited information regarding the station-satellite geometry. Basically, the carrier-phase observations only provide information about the change in the station-satellite geometry between observation epochs. This lack of information may be overcome – to a certain extent – by ensuring that the satellites are always observed by multiple ground stations. Complete loss of tracking of a satellite, even for only a few epochs, would mean that all the carrier-phase observations will be reset, and thus new ambiguity parameters will have to be estimated. This not only weakens the solutions with regard to orbital parameters, but also makes it impossible to solve for the transmitter clock offset during the outage.

An interesting question is how many stations are needed to obtain an acceptable high-accuracy solution. The response is driven by the following considerations:

- *Accuracy*: while additional stations in principle improve the accuracy and robustness of the solution, there is a point of marginal return given the precision of the measurements and redundancies in the tracking geometry (we expect accuracy to improve as a function of $\sqrt{n}$, where n is the number of observations).
- *Computational expense*: more stations lead to longer computation times, typically increasing by a factor of p^2, where p is the number of estimated parameters. This is a key consideration for services with stringent latency requirements, as fewer stations allow for faster processing.
- *Station costs*: more stations mean more costs for equipment installation and data transmission. This is an important factor for services relying on pro-

prietary networks (GNSS operators and commercial providers).

To investigate the impacts of the size of the network, we computed GPS POD solutions for eight consecutive days using real data from a network of 20 to 100 stations in steps of five. The obtained orbit quality was determined by comparing the resulting orbit to the IGS final orbit for the days in question. Figure 34.1 plots the median of the (absolute) residuals of the orbit differences as a function of the number of stations that were used in the solution. When increasing the number of stations, we kept the previous network and added new stations.

The results in Fig. 34.1 indicate that 60 stations should be sufficient to reach IGS orbit quality. A further increase in the number of stations does not significantly improve the orbit quality, at least not as reflected in the median of the squared residuals. So we may conclude that 60 stations are sufficient to achieve the accuracy of the IGS Rapid or Final products, as long as the tracking network is sufficiently well distributed to track all satellites from at least a handful of stations at any given epoch.

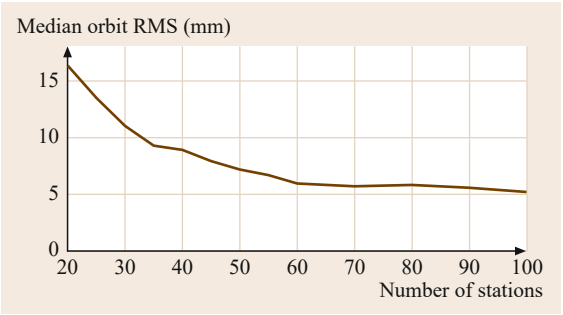

Fig. 34.1 Relation between the number of stations and the satellite orbit quality compared to the final orbits of the IGS

34.2 Models

GNSS software developers are well aware of meter level corrections that must be applied to range observations to eliminate effects such as special and general relativity, clock offsets, and atmospheric delays. All these effects are quite large, exceeding several meters, and must be considered even for pseudorange-only applications. When combining satellite positions and clocks precise to a few centimeters with ionospheric-free carrier-phase observations (few millimeter resolution), it becomes important to apply additional corrections that may not need to be considered in pseudorange or even differential phase processing.

This section describes relevant models given in the IERS conventions [34.2], followed by discussions of antenna phase center calibrations and key parameters related to the GNSS spacecraft. An overview of the important models is given in Table 34.1. References to sections of this handbook with more detailed information are given in the right column.

34.2.1 Reference Frame Transformation

The orbit dynamics of GNSS satellites is usually modeled in an Earth-centered inertial (ECI) frame (Sect. 3.2). However, station and satellite positions are conventionally expressed in an Earth-centered Earth-fixed (ECEF) reference frame, so a transformation between the ECI and the ECEF frame is necessary. This transformation is traditionally composed of three components (Sect. 2.5):

- Precession and nutation
- Polar motion
- UT1 and length of day (LOD).

In global GNSS solutions, precession and nutation are modeled with the IAU2000A R06 model, whereas polar motion and LOD are usually estimated (Sect. 34.4.6). UT1 cannot be determined by GNSS due to correlations with cross-track components of estimated orbital elements [34.3]. As a consequence, UT1 is fixed to values determined by very long baseline interferometry (VLBI) published in the *Bulletin A* [34.4] or the IERS C04 series [34.5]. As polar motion and LOD parameters are usually estimated with a temporal resolutions of 1 day, subdaily variations in these parameters mainly caused by ocean tides have to be considered with a specific model (Table 34.1).

34.2.2 Site Displacement Effects

Terrestrial stations undergo periodic movements (real or apparent) reaching a few decimeters that are not included in linear terrestrial reference frame (TRF) position models. Details are given in Chap. 2. Since most of the periodic station movements are nearly the same over broad areas of the Earth, they nearly cancel in relative positioning over short (< 100 km) baselines. However, to obtain precise station coordinates consistent with ITRF conventions with longer baselines or undifferenced processing, such station movements must

Table 34.1 Common correction models for GNSS data processing. IERS2010 refers to the International Earth Rotation and Reference Systems Service (IERS) conventions (2010). GPT = Global Pressure and Temperature (model); GMF = Global Mapping Function; VMF = Vienna Mapping Function; PCV = phase center variations; PCO = phase center offset; DCB = differential code bias

Model component	Maximum effect	Model	References
Nutation	±19 as	IAU2000A R06	Sect. 2.5
Subdaily polar motion	±1 mas	IERS2010	[34.2]
Subdaily length of day	±0.7 ms	IERS2010	[34.2]
Plate motion	Up to 1 dm/y	IGb08	[34.6]
Solid Earth tides	Up to 40 cm	IERS2010	[34.7], Sects. 2.3.5, 25.2.3
Ocean tidal loading	1–10 cm		[34.8], Sect. 25.2.3
		FES2004	[34.9]
		FES2012	[34.10]
Solid Earth pole tide	Up to 25 mm	IERS2010	Sects. 2.3.5, 25.2.3
Ocean pole tide loading	Up to 2 mm	IERS2010	[34.11]
Atmospheric tidal loading	Up to 1.5 mm	IERS2010	[34.12]
Troposphere (hydrostatic)	≈2.3 m[a]		Sects. 6.2.3, 19.3.2, 25.2.1
		GPT/GMF	[34.13, 14]
		GPT2	[34.15]
		VMF1	[34.16]
Ionosphere (1st order)	Up to 30 m[b]	LC[c]	Sects. 6.3.5, 19.3.1, 25.2.1
Ionosphere (higher order)	0–2 cm	IERS2010, IGRF11[d]	[34.17], Sect. 25.2.1
Relativistic corrections	Up to ±7 m[e]	IERS2010	[34.18], Sects. 5.4, 19.2
Satellite antenna z-offsets	0.7–2.7 m	`igs08.atx`	[34.19], Sect. 25.2.2
Satellite antenna PCVs	Up to 12 mm	`igs08.atx`	[34.19], Sect. 19.5
Receiver antenna PCOs	Up to 16 cm	`igs08.atx`	[34.19], Sect. 19.5
Receiver antenna PCVs	Up to 3 cm	`igs08.atx`	[34.19], Sect. 19.5
Phase wind-up	few cm	[34.20]	Sects. 19.4.1, 25.2.2
GPS satellite L1 C/A P(Y) DCBs	Up to 1 m	cc2noncc[f]	Sect. 19.6.1
Attitude	±180°[g]		[34.21], Sect. 3.4
		GPS: [34.22, 23]	
		GLO: [34.24]	
		BDS: [34.25]	
		QZS: [34.26]	
Albedo	1–2 cm[h]	[34.27]	Sect. 3.2.2
Antenna thrust	5 mm[i]	[34.28, 29]	[34.27]
Gravity field	3 km[j]	EGM2008	[34.30]

[a] In the zenith direction
[b] In the zenith direction for GPS L1 frequency
[c] LC is the ionosphere-free linear combination of dual-frequency observations (Sect. 20.2.3)
[d] International Geomagnetic Reference Field [34.31]
[e] Eccentricity correction for satellite clocks (largest effect)
[f] Available at http://acc.igs.org/
[g] Affects phase center location (instantaneous attitude error) and phase wind-up (accumulated attitude error)
[h] For GPS
[i] For GPS Block IIA
[j] Orbit error after two GPS revolutions when neglecting potential terms > 0 (Sect. 3.2)

be considered. This is accomplished by adding the site displacement correction terms to the linear nominal coordinates. The most significant corrections are summarized next.

Solid Earth Tides

The *solid* Earth is deformed due to the gravitational forces of the Sun and Moon. These solar and lunar tides cause periodic vertical and horizontal site displacements, which can reach about 30 cm and 5 cm in the radial and horizontal directions, respectively (Sect. 2.3.5). There is a latitude-dependent permanent displacement and a periodic displacement with predominantly semidiurnal and diurnal periods of changing amplitudes (Fig. 34.2). The periodic part is largely averaged out for static positioning over 24 h. The permanent part, however, remains. Even when averaging over long periods, neglecting this effect in point positioning would result in systematic position errors of up to 12 cm and 5 cm in the radial and horizontal directions, respectively.

The solid Earth tides may be represented by spherical harmonics of degree and order (n, m) characterized by the Love number h_m and the Shida number l_n. The effective values of these numbers weakly depend on station latitude and tidal frequency, which need to be taken into account when a millimeter-level position solution is desired. Note that the estimated ITRF station positions are corrected for the (conventional) permanent part of the solid Earth tides, resulting in a so-called *conventional* coordinate system.

Tidal Ocean Loading

Ocean loading results mainly from the load of ocean tides on the Earth's crust and is dominated by diurnal and semidiurnal periods (Fig 34.3). Displacements due to tidal ocean loading are almost an order of magnitude smaller than those due to solid Earth tides. Tidal ocean loading is also more localized, and by convention does not have a permanent component. Tidal ocean loading effects can be modeled for any station using the software package provided with the IERS conventions [34.2]. Computation of the station-specific loading effects using HARDISP requires the amplitudes and phases for the radial, south (positive), and west (positive), directions. The amplitudes and phases for any site may be obtained from the on-line ocean loading service of Chalmers University [34.32].

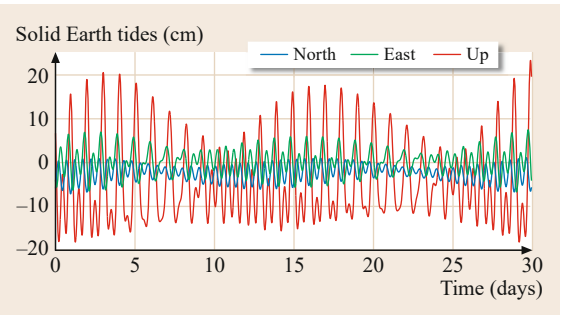

Fig. 34.2 Deformations due to solid Earth tides at Wettzell, Germany

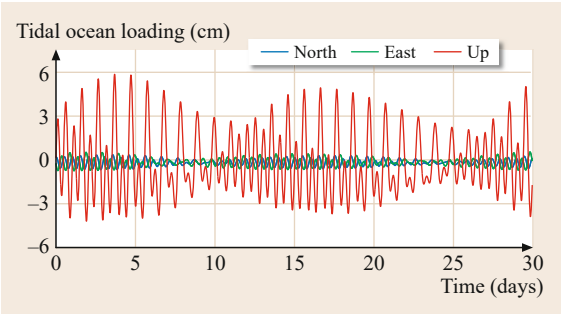

Fig. 34.3 Deformations due to tidal ocean loading at O'Higgins, Antarctica

Typically, the M2 amplitudes are the largest and do not exceed 5 cm in the radial and 2 cm in the horizontal directions for coastal stations. For centimeter precision, one should use a recent global ocean tide model, such as FES2004, EOT11a, FES2012, or newer. It may even be necessary to augment the global tidal model with local ocean tides digitized, for example, from local tidal charts. The station-specific amplitudes and phases may also include subdaily center-of-mass (CoM) tidal variations. In that case, ocean loading corrections have to be included for all stations regardless of proximity to an ocean. To be consistent with the subdaily Earth orientation parameter (EOP) convention, the IGS includes subdaily tidal CoM in ocean loading corrections when generating IGS POD solutions.

Pole Tides

Changes in the Earth's spin axis with respect to its crust, that is, the polar motion, cause periodical deformations due to minute changes in the Earth centrifugal potential. The variation of station coordinates caused by the pole tide can amount to around 2 cm and therefore needs to be taken into account. Unlike solid Earth tide and ocean loading effects, the pole tides do not average to nearly zero over 24 h. They are slowly changing according to the polar motion, and predominately vary at seasonal and Chandler (430 days) periods. Polar motion can reach up to 0.8 as and the maximum polar tide displacements can be up to 25 mm in height and 7 mm in the horizontal directions [34.2].

Ocean Pole Tides

The ocean pole tide is generated by the centrifugal effect of polar motion on the oceans. Polar motion is dominated by the 14-month Chandler wobble and annual variations. At these long periods, the ocean pole tide is expected to have an equilibrium response, where the displaced ocean surface is in equilibrium with the forcing equipotential surface. A self-consistent equilibrium model of the ocean pole tide is presented in [34.11]. This model accounts for continental boundaries, mass conservation over the oceans, self-gravitation, and loading of the ocean floor. The load deformation vector is expressed in terms of radial, north, and east components and is a function of the wobble parameters. Given that the amplitude of the wobble parameters is typically of order 0.3 as, the load deformation is typically no larger than about (1.8, 0.5, 0.5) mm in the (radial, north, east) components.

Tidal Atmospheric Loading

The diurnal heating of the atmosphere causes surface pressure oscillations at diurnal S1, semidiurnal S2, and higher harmonics. These atmospheric tides induce periodic motions on the Earth's surface [34.33]. The maximum amplitude of the vertical deformation is 1.5 mm for both the S1 and the S2 component. Being close to the orbital period of the GPS satellites, modeling of the S2 effect is especially important in order to minimize aliasing into dynamic parameters [34.34]. The IERS2010 conventions recommend calculating the station displacement using the S1 and S2 tidal model given by [34.12] (Fig. 34.4). As of 2015, not all IGS analysis centers apply tidal atmospheric loading models but this will likely be harmonized in time for the next IGS reprocessing campaign.

34.2.3 Tropospheric Delay

The nondispersive delay imparted by the atmosphere on a radio signal up to 30 GHz in frequency reaches a magnitude of about 2.3 m in the zenith direction at sea level [34.35]. It is conveniently divided into hydrostatic and wet components. The hydrostatic delay is caused by the refractivity of the dry gases (mainly N_2 and O_2) in the troposphere and by most of the nondipole component of the water vapor refractivity. The rest of the water vapor refractivity is responsible for most of the wet delay. The hydrostatic delay component accounts for roughly 90% of the total delay at any given site globally, but can vary between 80 and 100% depending on location and time of year. The relation between the delay at zenith direction and the actual observation direction is given by a mapping function (Chap. 6). Common mapping functions are the empirical Global Mapping Function (GMF, [34.14]) and the Vienna Mapping Function 1 (VMF1, [34.36]).

The hydrostatic delay can be accurately computed a priori based on reliable surface pressure data using the formula of [34.37] as given by [34.38]. One source for pressure data are the Global Pressure and Temperature (GPT) model and its successor GPT2 [34.13, 15]. Another possibility is the use of troposphere zenith delays derived from numerical weather models. Global grids with a spatial resolution of 2.0°×2.5° and a temporal resolution of 6 h obtained from European Centre for Medium-Range Weather Forecasts (ECMWF) data are provided together with the VMF1 coefficients.

There is currently no simple method to derive an accurate a priori value for the wet tropospheric delay, although research continues into the use of external monitoring devices (such as water vapor radiometers) for this purpose. Thus, in precise applications the residual zenith delay is usually estimated. Likewise, horizontal troposphere gradient parameters, needed to account for a systematic component in the North/South direction, are estimated rather than modeled (Sect. 34.4.3).

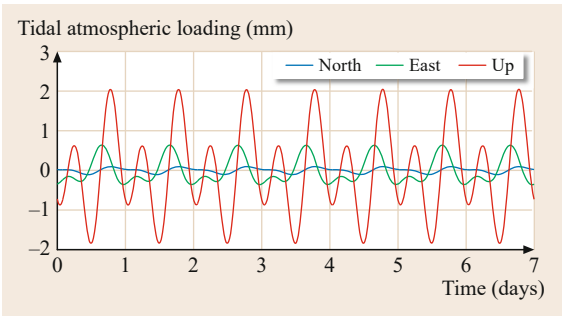

Fig. 34.4 Deformations due to tidal atmospheric loading at Fortaleza, Brazil

34.2.4 Ionospheric Delay

GNSS signals are refracted by free electrons and ions in the ionosphere, causing the signals to bend and change speed as they traverse this region. The ionization is caused by rays from the Sun and depends strongly on local time and solar activity. The signal delay due to the ionosphere can vary from meters to tens of meters depending on the ray path and ionospheric activity [34.35]. The delay is dispersive and may be eliminated to first order by linearly combining observations on two or more frequencies (with the side effect of increasing measurement noise, Sect. 20.2.3).

The second-order ionospheric effect can be removed using total electron content (TEC) estimates based on tracking data, an estimated global ionosphere model (GIM), or a climatological model such as the

International Reference Ionosphere [34.39]. The effect can be as large as a few centimeters and should be considered in precise GNSS analyses. An important impact of modeling second-order ionospheric delays is on the recovered terrestrial reference frame, which experiences an apparent southward shift of station coordinates of up to a few millimeters [34.40, 41]. For TRF comparisons spanning several years, this can equate to just over 1 cm in the Helmert transformation z-translation component at the fit epoch [34.42]. Other TRF transformation parameters are negligibly affected. There is also a small impact to satellite orbit positions (a few millimeter shift that is latitude dependent) and up to a 1 cm difference in the transmitter clock estimates [34.43]. Third-order ionospheric delay effects accumulate due to small path differences between signals at different frequencies. These can reach 1 mm in magnitude and are typically ignored in contemporary GNSS processing [34.17, 44]. Another ionospheric effect that is neglected by most IGS ACs is related to ray bending (excess path length) although it can reach a few millimeters at low elevations [34.2].

34.2.5 Relativistic Effects

Relativistic effects relevant for GNSS can be separated into three categories:

- Orbit effects (Sect. 3.2.2)
- Clock effects (Sect. 5.4)
- Propagation effects (Sect. 19.2).

The largest effect is a periodic transmitter clock variation caused by the noncircular orbits of the GNSS satellites. As a result, the satellites' speed and gravitational potential vary with orbital position, introducing a once-per-revolution variation of the transmitter clock with an amplitude of about 23 ns for a GPS satellite with an eccentricity of 0.01 [34.45]. In GNSS POD processing (including IGS products) this effect is modeled by convention, so the published transmitter clocks do not include this term. Smaller effects due to the oblateness of the Earth [34.46] and higher order terms of the Earth's gravity field are usually not considered for the product generation.

34.2.6 Antenna Phase Center Calibrations

Antenna calibrations are critical to high-accuracy GNSS processing. The calibrations define the points in space at which the electromagnetic ranging signal emanates from the transmitter antenna and induces voltage in the receiver antenna. In other words, the measurement geometry refers to the electrical phase centers. These are a function of local azimuth and elevation, frequency, and pseudorange or carrier phase (i. e., group or phase delay). Phase center calibrations are typically separated into a phase center offset (PCO, mean of the total calibration) and a phase center variation (PCV), which varies as a function of azimuth and elevation. In the IGS, absolute calibration standards have been adopted since 2006 [34.47]. The reader is referred to Chap. 17 and Sect. 19.5 for more details.

The transmitter calibrations are needed to refer range measurements to the spacecraft CoM. This is an important link because in POD the modeled spacecraft dynamics and estimated orbits refer to the CoM. The corresponding clock estimates, however, refer to the transmitter antenna phase center. Hence a user of precise products must apply antenna calibrations consistent with those used in the POD solution in order to realize the best accuracy.

Antenna calibration models are closely related to TRF implementation in POD. This is because antenna PCOs in the radial direction for both transmitters and receivers are not separable from TRF scale. IGS standard transmitter antenna calibrations are estimated while keeping scale fixed to a particular ITRF realization. The calibrations are estimated in global POD solutions, with receiver antenna positions fixed to the ITRF and ground calibrations fixed to absolute test range measurements [34.47]. In this manner, the TRF scale is handed off to the transmitter calibrations. It is therefore necessary to apply antenna calibrations consistent with the desired ITRF realization in POD solutions. Furthermore, a consistent set of calibrations must be derived for each version of the ITRF.

34.2.7 Phase Wind-Up

GNSS satellites transmit circularly polarized radio waves, so the observed carrier-phase depends on the mutual orientation of the satellite and receiver antennas. A full rotation of either the receiver or transmitter antenna around its boresight axis will change the carrier-phase measurement by one cycle. This effect is called *phase wind-up* [34.20]. A static receiver antenna remains oriented toward a fixed reference direction (usually north), but the motion of the transmitter relative to its boresight induces wind-up. Furthermore, the transmitter antennas rotate as the satellites yaw about their Earth-pointing axis (coincident with the antenna boresight, see Sect. 34.2.8).

During a satellite eclipse, the rotation can reach up to one revolution within half an hour. Consequently the phase data should be corrected for the wind-up effect. If wind-up is neglected in POD processing, the unmodeled change in carrier phase is absorbed as much as possible in unrelated parameters (Sect. 34.2.8).

34.2.8 GNSS Transmitter Models and Information

High-accuracy POD requires knowledge of and models for many satellite system parameters. These include satellite attitude, physical spacecraft geometry and material properties, operational information regarding the pseudo-random noise (PRN) codes transmitted by each space vehicle, maneuvers, and satellite health.

Spacecraft Attitude

POD requires knowledge of the satellite's attitude to relate range measurements from the antenna phase center to the spacecraft CoM using known antenna calibrations in the spacecraft body system. Nominal GNSS attitude control is guided by two constraints: pointing the transmit antenna toward the Earth's center, and pointing the solar panels, which rotate about their longitudinal axis, toward the Sun in order to obtain maximum energy transfer (Sect. 3.4). As discussed in [34.21], the IGS commonly adopts a right-handed spacecraft coordinate system where the body-fixed z-axis is aligned with the antenna boresight direction, where the y-axis points along the solar panel longitudinal axis, and x completes the right-handed set. Typically, the z-axis is controlled to point to the center of the Earth and the y-axis is kept perpendicular to the Sun direction. Within this so-called yaw-steering mode [34.48], the yaw angle Ψ is the angle between the x-axis of the spacecraft and the along-track direction (or, approximately, the velocity vector $\boldsymbol{v}$). This geometry is illustrated in Fig. 34.5.

To maintain nominal attitude, the spacecraft yaws about its z-axis and rotates the solar panels about y as it traverses the orbit. Because the solar panels can only rotate by 180°, the satellite performs a yaw maneuver at orbit noon and midnight (represented by μ equal to 180° and 0° when the spacecraft is closest and furthest from the Sun, respectively) so the solar panels can track the Sun for the next semi-orbit. The rate of the noon and midnight yaw maneuvers depend on the elevation of the Sun above the orbital plane of the GNSS satellite, commonly referred to as β (Fig. 34.5). The smaller β, the faster the satellite has to maneuver to maintain nominal attitude.

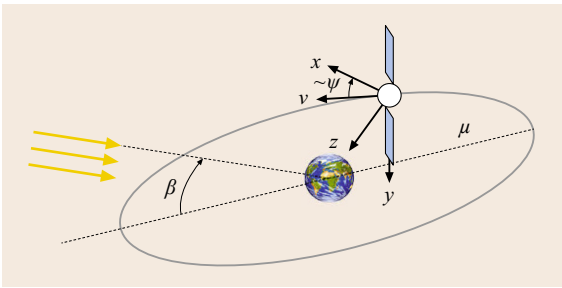

Fig. 34.5 Illustration of spacecraft body-fixed coordinate system and yaw attitude

Due to hardware limitations, GNSS satellites cannot maintain nominal attitude for small β angles. Spacecraft attitude control during these periods differs for each GNSS and even for satellite types within a GNSS. Correct attitude modeling is important because mismodeled yaw attitude in principle introduces errors in all estimated parameters. Mismodeled attitude in particular affects transmitter clock estimates because yaw maneuvers induce phase wind-up that is essentially common to all stations observing a satellite and therefore induces a clock-like effect. Detailed descriptions of the GPS, GLONASS, Galileo, BeiDou, and Quasi-Zenith Satellite System (QZSS) attitude models are found in Sect. 19.4.2.

Spacecraft Structure

Space vehicle geometry and material properties relate to dynamic force models. After gravity from the Earth, Moon, and Sun, solar radiation pressure (SRP) is the third largest force acting on a satellite orbiting the Earth at GNSS altitudes (Chap. 3). The magnitude and direction of the SRP depends on the satellite attitude and the spacecraft's structural geometry and material properties. Several approaches for dealing with SRP have been devised.

One approach is to solve for empirical accelerations representing SRP and other unmodeled forces in each orbit solution. This strategy originated at the Center for Orbit Determination in Europe (CODE), one of the IGS ACs, and is discussed further in Sect. 34.4.4 below.

A second approach is to generate an empirical SRP model from dynamic fits to precise orbits. The result becomes a background model in POD solution which then estimate only tightly constrained correction factors. The Jet Propulsion Laboratory (JPL) GNSS solar pressure model follows this approach to formulate Fourier expansions representing acceleration due to SRP as a function of the spacecraft type, orbit plane β angle, and satellite orbit angle μ [34.49, 50].

A third approach is to apply ray-tracing techniques to the spacecraft structure and optical material properties. Published models include early work by [34.51], resulting in a set of *ROCK* models for GPS Block I/II, as well as work by [34.52] for the GPS IIR spacecraft. Ray-tracing approaches are attractive because they promise to isolate the effects of SRP from other nonconservative forces, but are burdened by heavy computational loads for their generation and typically limited access to precise physical property information for the GNSS spacecraft.

In addition to SRP, POD nowadays requires modeling of forces on the GNSS spacecraft from optical and infrared Earth radiation, or Earth albedo [34.53]. Albedo radiation explains about half of the few-centimeter height biases seen between radiometric orbits and satellite laser ranging (SLR) measurements [34.54]. Currently all IGS ACs implement albedo visible and infrared models. Most use a model developed by [34.55] that computes albedo forces as a function of spacecraft type, position, time, and Sun position based on measurements of Earth radiation made by the Clouds and the Earth's Radiant Energy System (CERES, [34.56]). The forces due to albedo are largest in the radial orbit component.

Antenna Thrust

GNSS transmitters emit electromagnetic signals with total transmit powers upward of 70 W [34.29]. This results in a *recoil* acceleration in the orbit radial direction, which is now modeled by most IGS ACs, at least for GPS and GLONASS [34.52]. While the impact can be absorbed by an empirical acceleration parameter, modeling this physical effect in principle improves the recovery of transmitter phase centers and clock offsets since these parameters are correlated with antenna thrust.

Operational Information

Operational GNSS information is also needed for POD of GNSS satellites. Receivers typically identify the observations of tracked satellites by the number of their PRN code or the orbital slot number (for GLONASS). However, they do not know the relation between a given PRN/slot and the physical spacecraft, which may vary over time. Complementary knowledge of the unique space vehicle number (SVN) is required for POD because it defines characteristics including attitude control mechanisms, solar pressure and Earth radiation response, clock properties, antenna calibration, signal types, and emitted power. PRN/SVN assignments are tracked by the IGS ACs based on information provided by the GNSS system operators where available (see, e.g., the constellation status websites summarized in Table 34.2).

Knowledge of satellite health status over time, as extracted from the navigation message, is needed because unhealthy periods may indicate payload maintenance, orbit maneuvers, or nonstandard signal transmission. One typically excludes unhealthy satellites from low-latency, automated processing (e.g., ultra-rapid and rapid) to ensure reliable product delivery, but several IGS ACs include unhealthy satellites in their final products as long as all quality metrics are satisfied. This approach is possible because sometimes satellites are marked unhealthy for reasons unrelated to the navigation signal performance. Such unhealthy periods are usually announced in advance by the GNSS system operators via a so-called Notice Advisory (Table 34.2).

Table 34.2 Constellation status and notice advisories for GPS, GLONASS, Galileo, and QZSS. For BeiDou no such official information is available as of early 2016

GNSS	Item	Reference
GPS	Status	[34.57]
	NANU[a]	[34.58]
GLONASS	Status	[34.59]
	NAGU[b]	[34.60]
Galileo	Status	[34.61]
	NAGU[c]	[34.62]
QZSS	Status	[34.63]
	NAQU[d]	[34.64]

[a] Notice Advisory to NAVSTAR Users
[b] Notice Advisory to GLONASS Users
[c] Notice Advisory to Galileo Users
[d] Notice Advisory to QZSS Users

34.2.9 Models in Downstream Applications

It is important to apply consistent models in POD processing and downstream applications utilizing POD products (e.g., precise point positioning (PPP), Chap. 25). In particular, inconsistent antenna calibration and satellite attitude models can result in measurement model errors, which will be absorbed by estimated parameters to the extent possible. The remaining misfit will be evident in postfit residuals. The risk of contaminating physical parameters of interest is, therefore, significant. For this reason, GNSS software providers recommend using POD products generated with the same software as this reduces the likelihood of inconsistent models.

34.3 POD Process

The POD process consists of several discrete steps leading from raw observations through data editing and measurement modeling to parameter estimation and product generation. A high-level diagram showing the connected steps is shown in Fig. 34.6. The top row depicts needed inputs, including raw observation data (typically in Receiver INdependent EXchange (RINEX) format, Annex A.1.2), nominal GNSS orbits/clocks, and EOPs. Satellite and station metadata (PRN/SVN conversions, spacecraft models, nominal station coordinates, antenna information, etc.) are needed at various steps and are not explicitly depicted.

Item 1 in the figure represents the data editing procedure, which evaluates the raw observations and linear data type combinations (e.g., range minus phase, widelane phase, see Chap. 20) to identify poor quality observations (such as very short arcs, inconsistent range/phase) and carrier-phase cycle slips. If the nominal orbits and clocks are of good quality, then data for each station may be edited using a PPP procedure that includes editing based on raw observations as well as iterative editing based on postfit residuals. The latter approach is generally possible if an ultra-rapid or better nominal orbit and clock product is used as input, and has the advantage of identifying data to remove for each station independently. When postfit residual editing is performed in a global solution, there is some risk that poor quality or nonsensical observations from one station impact postfit residuals across many stations since the global estimation process adjusts parameters to minimize postfit residuals (in a least-squares sense) over all network participants.

Item 2 employs an orbit integrator to generate a dynamic fit to a set of nominal orbits. The nominal orbits could come from the broadcast ephemerides, prior precise solutions, or predictions of past precise orbits to span the processing arc. The dynamic fit is performed iteratively to minimize the difference between the es-

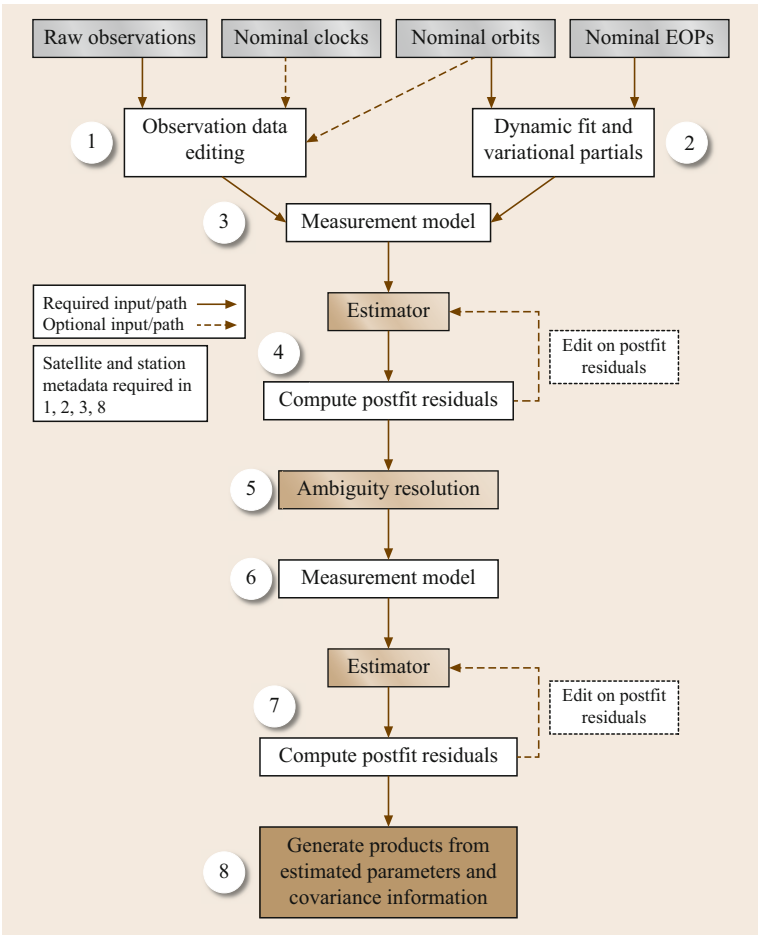

Fig. 34.6 High-level overview of the POD process (representative example)

timated and the nominal orbits using a small set of parameters (at least the epoch state vector or orbital elements as well as a limited number of SRP parameters). The difference between the nominal and generated dynamic orbits reflects both the accuracy of the nominal orbits and the number of fitted parameters. Significant misfits can be used to screen for model errors and satellites not following a sufficiently dynamic trajectory due to, for example, orbit maneuvers or unusual attitude configurations. This step also computes the partial derivatives of the position and velocity vectors with respect to the orbit parameters (variational partials).

The measurement model, labeled as item 3, computes the expected measurements corresponding to the input set of observations (item 1). These are based on instantaneous nominal receiver and transmitter antenna phase centers determined from nominal values and the models described in Sect. 34.2. Since the GNSS measurements (observations) have nonlinear relationships to the estimated parameters (state variables), the observation-state equations are linearized about the nominal state. The computed measurements are subtracted from the observations at this step, and the partial derivatives of the linearized measurement model with respect to the estimated parameters are determined.

The variational partials and outputs of the measurement model are then passed to an estimator that adjusts parameters to minimize a cost function such as the sum of the square of the postfit residuals (item 4). The estimator solves for an adjustment to the nominal state that best fits the observations, typically iterating the solution until the adjustment is smaller than some threshold (i. e., convergence). This works as long as the nominal state and the estimated state fall within the linear regime of the observation–state relationships. The estimator solution is the sum of the nominal and adjusted parameter values.

The set of estimated parameters usually includes the following: station coordinates, station troposphere delays, transmitter satellite orbits (epoch state, empirical accelerations and/or solar pressure model scales), EOPs, receiver and transmitter clocks, floating point, and integer fixed carrier-phase ambiguities. When more than one GNSS is used, receiver intersystem biases and/or interfrequency biases (IFBs) are additionally estimated. The outputs of the estimator include the parameter adjustments, estimated covariance, and postfit residuals. The residuals may be examined for outliers, and the solution iterated using successively smaller residual outlier thresholds.

The results of this step also provide the input for the subsequent carrier-phase integer ambiguity resolution (item 5, see Sect. 34.4.7 and Chap. 23). After ambiguity resolution, the measurement model is run again to account for resolved integers in the observations (item 6), after which the ambiguity resolved estimator solution is generated (item 7). Here, too, one can iteratively edit observations based on postfit residuals, although almost all outliers should have been removed in prior iterations. The estimated parameters and covariance information is then used to create product files (item 8) for distribution to the users.

34.4 Estimation Strategies

Various estimation strategies are used within the IGS POD community. Some analysis centers process undifferenced pseudorange and carrier-phase observations and estimate all parameters in one integrated solution. Others process double-difference carrier-phase observations, which remove clock parameters from the measurements, and solve for orbits, EOPs, station positions, tropospheric delays, and carrier-phase integer ambiguities. The estimates can then be held fixed in a follow-on solution that uses undifferenced observations to solve for clock parameters consistent with the double-difference solution. The processing arcs found within the IGS range from 24 h to 3 days. Longer arcs are preferred for orbit parameters since additional revolutions improve knowledge of the dynamics. A 1-day arc is preferred for EOP and station position parameters if a daily terrestrial reference frame is of interest. Carrier-phase observations are usually weighted at least 100 times higher than pseudorange due to their significantly higher precision (e.g., 1 cm and 1 m, respectively). Sometimes data from individual stations are also weighted according to the overall root mean square (RMS) level of their postfit residuals in an initial solution, since relatively high postfit residuals may indicate issues with model fidelity or data editing at particular locations. In the following subsections, we describe common estimators, parameterizations, and strategies for additional aspects of POD in further detail.

34.4.1 Estimators

In the IGS community, two primary types of estimators are utilized for GNSS orbit and clock determination. The first is the batch least-squares estimator, which takes all observations, partial derivatives, and a priori covariance for the processing arc to form

a normal equation system that is inverted to compute state variable adjustments and covariance information (state variable uncertainties and correlations). The second category comprises sequential estimators (such as the Kalman or square root information filter [34.65]), which ingest observations one epoch at a time to produce the best state adjustment based on measurements processed so far. Both types of estimators are discussed in detail in Chap. 22. We also refer the reader to [34.66, 67] for thorough reviews of filtering techniques in the context of range measurement processing.

A significant difference between the batch least-squares estimation and Kalman filtering lies in the treatment of stochastic, time-variable parameters [34.67]. In the case of the batch estimator, distinct estimation parameters need to be set up for each new epoch or time interval (e.g., a clock offset at each epoch, a zenith troposphere delay every hour, and daily station coordinates). This creates large normal equation matrices (Sect. 34.4.10), so parameter elimination and back-substitution techniques are used to reduce the computational burden [34.68]. For the Kalman filter, the number of parameters remains constant, but process noise is applied between epochs. The process noise can be configured to apply white noise (no correlation from estimate to estimate), colored noise (correlation over a period of time), or random walk (infinite correlation) updates to a parameter.

34.4.2 Parameterization

All state-of-the-art precise GNSS software packages make available a variety of parameterizations. The most common are as follows:

- *Offset*: adjusts a single, constant value over the processing arc. Commonly used for station coordinates since geodetic stations are considered static over processing arcs of up to several days. Also used for differential code biases (DCBs) (spanning up to monthly intervals) and antenna PCOs.
- *Piecewise-constant*: offset parameters with discrete steps. Typically used for carrier-phase ambiguities.
- *Piecewise-linear*: described by an offset and a slope. Typically used for EOPs.
- *Continuous piecewise-linear*: a piecewise-linear parameterization with imposed continuity at the interval boundaries. It is typically achieved by estimating the parameter values at discrete nodal points located at these boundaries. Compared to the piecewise-linear representation, the number of estimation parameters is reduced by $n-1$ with n being the number of time intervals. Equivalent to a piecewise-linear representation with a tight continuity constraint. No discontinuities occur inside the processing interval allowing for a more physical parameter representation. The piecewise-linear representation can be transformed to a continuous piecewise-linear representation but not vice versa. Used for station troposphere delays, EOPs in high-rate or multiday solutions, and nadir-dependent satellite antenna PCVs.
- *Epoch independent*: an independent parameter values is estimated at each epoch, for example, used for receiver and transmitter clocks. Equivalent to a constant parameter with a stochastic white noise reset applied at every epoch.

An illustration of these five types of parameterizations is shown in Fig. 34.7.

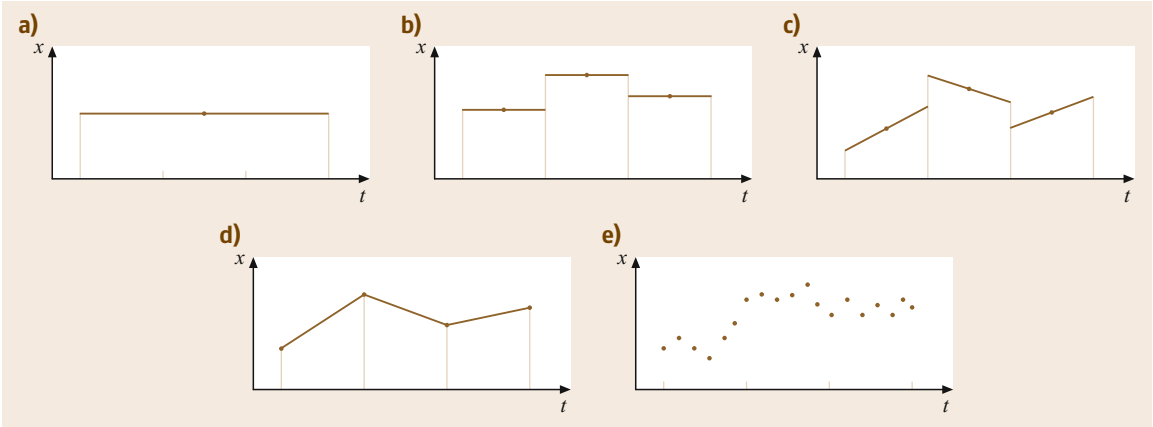

Fig. 34.7a–e Parameterizations used in GNSS data processing: **(a)** offset, **(b)** piecewise-constant, **(c)** piecewise-linear, **(d)** continuous piecewise-linear, **(e)** epoch independent

34.4.3 Ground Stations

For ground stations one must estimate coordinates, tropospheric delay, and receiver clock parameters. For geodetic stations, it is usually sufficient to estimate a constant position over the processing arc with loose a priori constraints in the range of meters to kilometers.

The troposphere is modeled using a zenith path delay, a mapping function which may vary by time and the station location (e.g., Global Mapping Function, [34.14]), and horizontal gradient parameters. Although the analysis of observations at low elevations is degraded by increased noise, multipath, and model deficiencies, these observations are important for a decorrelation of troposphere zenith delays, receiver clock, and station height ([34.69] and Fig. 6.3). Therefore, low-elevation data are included but downweighted. Common weighting functions are $1/\sin e$ and $1/\sin^2 e$ with the satellite elevation e, additional weighting functions are discussed in [34.70] and [34.71]. Nevertheless, data at very low elevations are excluded by applying an elevation mask. Typical elevation cut-off angles range from 3° to 10°.

Horizontal tropospheric gradient parameters are needed to account for a systematic component in the north/south direction toward the equator due to the atmospheric bulge [34.72] with magnitudes of about −0.5 and +0.5 mm at mid-latitudes in the Northern and Southern hemispheres, respectively. The gradients are generally parameterized for each station as components of a sinusoid varying in azimuth. The gradients also capture the effects of random components in both directions due to weather systems. Failing to model gradients in radiometric analyses can lead to systematic errors in the scale of the estimated terrestrial reference frame at the level of about 1 ppb, and cause latitude and declination offsets in station and transmitter positions [34.73].

The zenith path delay parameter may be estimated as a piecewise constant (random walk) process with an a priori sigma of tens of centimeters and process noise < 1 mm over 5 min (1σ). Likewise gradient parameters, usually the in-phase and quadrature components of an empirical sinusoid fit, may be modeled as random walk processes with similar a priori sigmas and process noise an order of magnitude smaller than the zenith delay. The estimation of receiver clock parameters is discussed in Sect. 34.4.5.

34.4.4 GNSS Orbits

The satellite orbits are estimated using a *reduced dynamic* approach [34.74]. The basic outline is to solve for an epoch state vector (position and velocity or set of osculating elements at a reference epoch), empirical accelerations and/or model scale factors to absorb force model errors (mainly solar radiation, Earth radiation, spacecraft thermal radiation, and transmitter antenna thrust), and, optionally, yaw attitude parameters. For SRP modeling, the strategies currently represented in the IGS analysis community may be broadly divided into two categories.

The first is the *CODE approach* described in [34.75, 76]. Here, one estimates an epoch state plus constant and per-revolution accelerations in the DYB-frame (where D refers to the spacecraft-Sun direction, Y to the body-fixed solar panel axis, and B completes the right-handed set). The classic ECOM (Empirical CODE Orbit Model) approach solves for 6 epoch state parameters and 5 empirical accelerations as constant terms in D, Y, and B and 1/rev terms in B (Sect. 3.2.4). In 2015, the CODE AC updated this strategy to also include two- and four-times per revolution accelerations in the spacecraft-Sun direction (ECOM-2), as this was empirically found to reduce signals related to the GNSS draconitic period seen in terrestrial reference frame transformation parameters [34.77].

The second category, developed at JPL, emphasizes high-fidelity a priori SRP models and estimates tightly constrained SRP model scale and empirical accelerations for each arc [34.49, 50]. A typical set of parameters is the epoch state, an overall constant solar pressure model scale factor, tightly constrained stochastic solar scale in the spacecraft body-fixed x- and z-components, plus constant and constrained stochastic accelerations in y (accounting for unmodeled thermal radiation and SRP forces).

Contemporary orbit solutions submitted to the IGS are derived using both approaches and variations thereof. They show agreement within the expected precision of the estimates. In other words, the approaches independently validate one another and produce high-quality solutions. There are, of course, some advantages and disadvantages for each. The CODE approach has the advantage that it requires no a priori model for SRP forces as they are simply absorbed by the empirical accelerations. It is therefore well suited to dealing with new spacecraft types as soon as tracking data are available. The disadvantage of the approach is that significant empirical forces must be estimated, and there is the risk of mixing dynamical parameters with other physical parameters such as EOPs and geocenter [34.77, 78].

The advantage of the second category is that the forces acting on the satellite are defined by a high-fidelity a priori model such that empirical accelerations can be tightly constrained to account for hopefully small deficiencies in the background models. This, in principle, allows for less mixing of spacecraft dynamics into other geodetic parameters. The disadvantage of

this approach is that it relies on a prior set of precise orbits (from which the SRP model is generated) so it cannot be readily applied to new satellites. Further, any systematic errors in the prior orbit set can affect the resulting SRP model.

The estimation of yaw rates for orbit shadow and noon maneuvers for the GPS Block II/IIA/IIF satellites is also beneficial. In the case of the Block II/IIA spacecraft, this is needed because the maneuver is controlled by analog sensors resulting in yaw rates that can differ from nominal values by as much as 25% [34.48]. While the Block IIF attitude is deterministic, nonetheless discrepancies between nominal and actual attitude for some β angle regimes have been found [34.24]. A new yaw parameter should be setup (or stochastic update performed) for each yaw maneuver since they are independent events. Analyses have shown that GPS Block IIR and GLONASS-M attitude may be accurately modeled without the need for empirical parameters [34.22, 24].

34.4.5 Clock Offsets

The next class of parameters are receiver and transmitter clock offsets. The clocks are generally modeled as unconstrained epoch-independent parameters (no correlation from one epoch to the next). This parameterization makes the solution independent of the quality of the individual station clocks, most of which are not tied to an atomic reference.

Transmitter clocks are driven by atomic frequency standards, but may exhibit discontinuities that make modeling them as, for example, a quadratic function unreliable. The solution is singular if all clocks are left unconstrained, so a reference must be selected. In practice this implies that one holds a particular clock offset or an ensemble of clocks fixed, meaning all other clock offsets are estimated relative to the reference. Generally one can use a station stably tied to a reference time scale such as the coordinated universal time (UTC) realizations of national timing labs.

An alternate approach less sensitive to data gaps is to apply an overall zero mean constraint to an ensemble of clock offsets. Some ACs, for instance, apply a zero-mean constraint to the transmitter clocks. The resulting orbit and clock solution is internally consistent and yields valid formal error estimates for all parameters. The timescale of the solution may be adjusted after the fact by removing a single reference clock offset at each epoch from all clock estimates based on a prioritized list of receiver clocks aligned to GPS time.

The GPS clock parameters provided by the IGS refer (by convention) to the ionosphere-free linear combination of the L1 P(Y) and L2 P(Y) signals. However, several geodetic GPS receivers only track the C/A code on L1. Therefore, DCBs between the different types of signals have to be considered (Sect. 19.6.1). One can either estimate the DCB parameters, as done by the CODE AC, or one can correct for the DCBs, for example, with the cc2noncc tool utilizing the CODE DCB estimates [34.79]. Users of IGS clock products must ensure consistency between the clock parameters on the one hand and the observation types on the other hand by applying the corresponding DCBs. Further sources for DCBs are the Time Group Delay (TGD) parameters of the GPS navigation message (Sect. 7.4.3), the Inter Signal Corrections (ISCs) of the GPS Civil Navigation Message CNAV [34.80], and the IGS MGEX DCB product [34.81].

34.4.6 Earth Orientation

Earth orientation parameters relate the terrestrial reference frame to the celestial reference frame. UT1–UTC measures the rotation rate of the Earth relative to an atomic time scale. The period of one Earth revolution is not constant in time, and rotation time in excess of 24 h is referred to as the length of day (LOD). Global GNSS solutions are sensitive to changes in the Earth rotation rate over a processing arc but not the absolute rotational alignment at the start of the arc. From the change in rotation one can compute LOD as described in [34.2]. The x- and y-coordinates of the Earth rotation axis, as well as their rates, can also be determined from GNSS. By convention the estimated pole coordinates are with respect to the IERS Reference Pole [34.2].

34.4.7 Phase Ambiguity Resolution

To achieve the best precision and accuracy, one should resolve phase measurement integer cycle ambiguities. Details on ambiguity resolution algorithms are provided in Chap. 23, here we focus on the steps taken in a global POD solution.

The process usually starts with a solution that estimates the float-valued ambiguities of the ionosphere-free combination of dual-frequency carrier-phase observations along with the station, troposphere, satellite orbit, clock, Earth orientation, and DCB parameters. For a daily solution with 60 or more well-distributed ground stations one can expect orbit accuracies around 10 cm (3D RMS) and clock accuracies of about 10 cm.

This accuracy is generally sufficient to facilitate ambiguity resolution in a second step, where the above parameters are introduced as known parameters (with given accuracy) to setup systems of equations for resolving double-difference ambiguities for individual pairs of stations. The specific techniques employed in

this step differ widely between analysis centers and software packages [34.82–84], although many of them are based on a widelane/narrowlane approach utilizing the Melbourne–Wübbena linear combination.

Given the wealth of observations available, it is usually best to apply conservative thresholds for accepting ambiguities. It is far better to resolve fewer ambiguities correctly than resolving more ambiguities and resolving an integer incorrectly. This is critical since the integers are introduced as fixed values in a follow-up estimation that effectively treats carrier-phase measurements as highly precise, unbiased ranges. Typically one can expect to resolve upward of 90% of ambiguities in a 60+ station global solution.

34.4.8 Multi-GNSS Processing

Although the orbital configurations of GLONASS, Galileo, and BeiDou satellites in medium Earth orbit (MEO) are similar to GPS, the existing estimation strategies partly fail for these satellites.

Systematic errors have been revealed at the 20 cm level in the Galileo orbit and clock products of four different ACs [34.85]. The stretched shape of the Galileo satellites have been identified as the root cause of these errors and an a priori box model has been developed, significantly reducing the systematic errors [34.86]. A similar orbit quality can also be achieved with the newly developed ECOM-2 model [34.77]. While spacecraft attitude and antenna phase centers differ for these satellites they can in principle be derived using procedures developed for GPS. POD of geostationary satellites as employed by BeiDou is still challenging due to the small changes in observation geometry and frequent maneuvers [34.87], although some progress has been made with alternative orbit parameterizations [34.88].

The estimation of clocks for these systems is also similar to GPS in that the offsets can be treated as unconstrained epoch-independent parameters. In a solution involving GLONASS several additional parameters are, however, needed. First, one must estimate a GLONASS intersystem bias at each receiver. GNSS receiver data typically refer the measurements to the respective system time, while the POD solution refers all estimates to GPS time (by convention). So an overall clock bias captures the difference between the GPS and GLONASS timescales at each receiver. It affects all GLONASS range and phase measurements equally. The estimated values should, in general, be in the vicinity of the GPS–GLONASS system time offset, which today is better than 1 μs after accounting for the constant 3 h UTC(USNO)–UTC(SU) bias [34.89].

A second set of additional parameters needed for GLONASS are IFBs along each receiver–transmitter pseudorange link. These link biases are necessitated by the frequency division multiple access (FDMA) architecture of the GLONASS system (Sect. 8.2.2), as the hardware delays experienced by GLONASS signals traveling through the receiving equipment are dispersive. The delays vary due to both the physical equipment as well as environmental factors such as temperature. A reasonable strategy is to estimate each IFB as a constant parameter over each day. Due to the estimation of IFB parameters, the choice of the reference signals for GLONASS clock estimation (e.g., P- or C/A-code) is arbitrary.

The magnitude of the IFB parameters is in the range of decimeters to 3 m depending on the receiver type [34.90]. One must choose a reference for both the system time offsets and IFBs or the solution is singular. One can fix to calibrated values or artificially set these biases to zero for a particular receiver. Either way the solution yields a consistent set of GPS and GLONASS clock offsets suitable for use in combined GPS/GLONASS point positioning; however one must take care to also estimate a GLONASS time offset and IFBs in that solution.

It is clear that the GLONASS clock estimates depend strongly on the choice of the system time offset and IFB reference, as well as the choice of receiver network in general since the IFBs essentially bias the pseudorange on each link (unlike GPS where IFBs are not needed since all signals are on common frequencies). For these reasons, it is quite complicated to compare GLONASS clock estimates from different solutions if a different reference and receiver networks were used. This is the main reason the IGS does not currently produce a GLONASS clock combination [34.91].

Galileo and BeiDou are code division multiple access (CDMA) systems like GPS. Thus, in a combined solution one only needs to estimate GPS to Galileo and/or BeiDou time offsets at each station, parameterized as an overall constellation bias (intersystem bias) over the processing arc. A key choice related to the bias magnitudes is the ionosphere-free observable type. For Galileo an E1/E5a convention is emerging [34.85], while for the BeiDou B1/B2 signals are used [34.92].

An important consideration in multi-GNSS solutions is the weighting of observations from each GNSS. Weighting observations in the same manner regardless of GNSS is of course one possibility. Two other commonly used approaches are to downweight observations from non-GPS constellations, or to derive station clock and troposphere parameters with GPS alone and hold the results fixed in a follow-on solution that estimates intersystem biases, transmitter clocks, IFBs, and satellite orbits for one or more additional constellations. This is beneficial since the satellite constellations and

ground networks for the other GNSSs are (currently) not as large or well distributed as for GPS. Also, detailed models for the newer constellations are still being developed and refined. This situation will change rapidly in the next few years and it is likely that new weighting strategies will emerge.

34.4.9 Terrestrial Reference Frame

A stable, accurate, and well-maintained global TRF is a prerequisite for precise orbit and clock determination and its applications. The TRF underpins POD by defining the origin from which receiver and transmitter locations are defined. It furthermore establishes the framework upon which geophysical processes, such as solid Earth tides or vertical motion due to ocean loading, are modeled and analyzed. Details on the definition and realization of terrestrial reference systems are given in Sect. 2.3.

The most recent version of the International Terrestrial Reference Frame is ITRF2008. However, ITRF2008 is usually not directly used in GNSS applications as the predecessor of the current antenna model was applied for the IGS contribution to ITRF2008. Therefore, a GNSS-only TRF called IGS08 was computed [34.6]. It is aligned to ITRF2008 but includes station-specific corrections to account for the antenna calibration differences. In 2012, an updated version of IGS08 called IGb08 [34.93] was released as the coordinates of more than 30 reference frame stations were degraded due to station displacements induced by earthquakes or equipment changes.

The TRF is realized in global POD solutions in one of three ways:

1. Fixing or tightly constraining a set of station positions to the values defined by the TRF. In principle, three fixed stations are sufficient, although in practice IGS ACs hold at least two dozen globally distributed stations fixed. The positions of the remaining stations in the solution, as well as the GNSS orbits, will therefore be estimated relative to the realization of the TRF defined by the subset of fixed stations. However, fixing or constraining more stations than necessary might result in distortions of the network geometry. This approach is typically used only for low-latency solutions (i. e., ultra-rapid) where realizing a TRF a posteriori is time consuming or not valuable for user applications.
2. Applying *minimum constraints* for a selected set of (core) stations w.r.t. the a priori TRF. For global GNSS solutions, a no-net-rotation condition is mandatory. If the origin of the tracking network (geocenter) is estimated, an additional no-net-translation condition has to be applied. The advantage of this approach is that the inner geometry of the network is not distorted.
3. Estimation of all station positions in the global solutions with loose a priori constraints. Other than relating to the TRF through antenna calibrations (discussed below), this type of *fiducial free* POD solution does not provide orbits and clocks in a particular TRF but instead realizes a unique frame for that solution. This solution's frame is likely to exhibit notable rotations with respect to ITRF because the GNSS technique is insensitive to rotating the entire observation geometry. One can compute a best fit Helmert transformation (Chap. 2) for the estimated ground network relative to ITRF using the set of overlapping stations (XYZ translations, XYZ rotations, and scale) and apply this transformation to the orbit solution to place it in the ITRF frame.

The products resulting from one of these approaches are provided in the underlying TRF and therefore directly transfer the TRF to users.

Due to orbit dynamics, the GNSS satellites orbits refer to the CoM of the total Earth system including the oceans and the atmosphere. Tides cause periodic variations in the CoM of the oceans and the atmosphere. This so-called geocenter motion can reach up to 1 cm for diurnal and semidiurnal ocean tides [34.94]. If a corresponding CoM correction (CMC) is applied, the orbits refer to a crust-based Center-of-Network (CoN) frame, otherwise to a CoM frame. Within the IGS, the CoN frame is used for the orbits as well as the clocks [34.95].

Table 34.3 Number of observations and estimation parameters in a global GPS solution with 32 satellites and 160 stations. It is assumed that 10 satellites are visible per station and observation epoch

	Sampling	No. of obs./par.
Observations	5 min	460 800
Station coordinates	24 h	480
Troposphere zenith delays	2 h	2080
Troposphere gradients	24 h	640
Orbit parameters	24 h	576
Earth orientation parameters	24 h	5
Ambiguities	Dep. on data	≈ 10 000
Satellite clocks	5 min	9216
Receiver clocks	5 min	46 080
Total number of parameters		≈ 69 000

34.4.10 Sample Parameterizations

Table 34.3 gives an overview of the estimated parameters and their sampling for a global GPS solution with

Table 34.4 Sample receiver station parameterization (JPL approach) (after [34.50])

Parameter	Configuration	σ_{apr}	σ process noise
Station coordinates (all or a subset of stations)	Offset	1 km	–
Station zenith wet troposphere	Random walk, 10 min updates	0.5 m	0.03 mm $s^{-1/2}$
Station gradient wet troposphere	Random walk, 10 min updates	0.5 m	0.003 mm $s^{-1/2}$
Station clock offset	White noise, update each epoch	1 s	1 s

Table 34.5 Sample satellite parameterization (CODE approach) (after [34.76, 96])

Parameter	Configuration	σ_{apr}
Keplerian elements at epoch	Offset	No constraint
Acceleration in the Sun-direction (D)	Offset	No constraint
Acceleration in the Y-direction	Offset	No constraint
Acceleration in the B-direction	Offset	No constraint
Acceleration in the B-direction (once per revolution)	Offset	No constraint
Constant radial velocity change	Every 12 h	$1 \cdot 10^{-6}$ m s^{-1}
Constant along-track velocity change	Every 12 h	$1 \cdot 10^{-5}$ m s^{-1}
Constant cross-track velocity change	Every 12 h	$1 \cdot 10^{-8}$ m s^{-1}

Table 34.6 Sample satellite parameterization (JPL approach) (after [34.50])

Parameter	Configuration	σ_{apr}	σ process noise
Position at epoch	Offset	1 km	–
Velocity at epoch	Offset	1 cm s^{-1}	–
Y acceleration	Offset	1 nm s^{-2}	–
Y acceleration	Colored noise, 4 h correlation, updated every 1 h	0.01 nm s^{-2}	0.0002 nm $s^{-2} s^{-1/2}$
SRP model scale	Offset	1.0	–
SRP model scale in X and Z	Colored noise, 4 h correlation, updated every 1 h	0.01	0.0002 $s^{-1/2}$
GPS Block II/IIA yaw rates	Offset per eclipsing midnight/noon turn	0.01 deg s^{-1}	–
Transmitter clock offset	White noise, update each epoch	1 s	1 s

a full constellation of 32 satellites and a network of 160 terrestrial stations at a 5 min sampling rate. Clock offsets make up the vast majority of parameters. These parameters are removed if double-difference measurements are processed. The next largest parameter group is for ambiguities whose number strongly depends on the data quality. Efficient methods to deal with the huge number of almost 70 000 estimation parameters are discussed in Sect. 34.4.11.

More specific sets of estimated parameters are discussed in the following. We list sample a priori standard deviations (σ) and stochastic properties, which provide reasonable solutions based on POD strategies described in [34.50, 75, 76]. We note that some software packages apply stochastic updates directly in a Kalman filter [34.67], while those using a batch filter typically configure a new (optionally constrained) parameter for each update and apply elimination techniques to the normal equations to reduce the computational burden. For the purposes of this discussion we consider both approaches to yield equivalent parameterizations. Table 34.4 shows a sample receiver station parameter configuration, Tables 34.5 and 34.6 show possible satellite parameterizations, and Table 34.7 refers to EOPs. Range and phase data are often given a priori measurement sigmas of 1 m and 1 cm, respectively, or a factor of 1:100, to give credit to the high precision of the carrier-phase measurements. This in effect produces a phase-based solution that aligns the clock estimates to the pseudoranges.

Table 34.7 Sample Earth orientation parameterization (JPL approach) (after [34.50])

Parameter	Configuration	σ_{apr}
X and Y pole	Offset	5 m (relative to a priori)
UT1-UTC rate per arc	Offset	$3.5 \cdot 10^{-8}$ s/s

34.4.11 Reducing Computation Cost

A given arc and dataset can of course be processed as one solution from start to finish. This approach is often taken to produce few-hour latency (ultra-rapid) or next-day (rapid) solutions. There are, however, trade-

offs between accuracy, processing time, and the number of stations and orbiters processed, as discussed in Sect. 34.1. A few strategies are commonly used to maximize the number of receivers and transmitters while minimizing processing time:

- Real-time clock estimation (few second latency) based on ultra-rapid orbits: GNSS orbits can be predicted from a precise solution with sufficient accuracy (over many hours and even days) that they may be input and held fixed in a real-time GNSS clock filter. This reduces the computational burden and complexity of the real-time process, which estimates only clock and troposphere parameters. This approach is widely used to produce real-time GNSS solutions [34.97].
- Reuse of normal equation systems from prior POD solutions: many software packages include tools to manipulate and stack normal equation systems, and take advantage of these capabilities to minimize new computations for low-latency processing. For instance, utilizing prior rapid or ultra-rapid normal equation systems and appending a few hours of new data to generate an ultra-rapid solution. This avoids recomputing the measurement model and partial derivatives for a significant portion of the dataset. Normal equation stacking is also an efficient tool to generate multiday orbital arcs.
- Stacking normal equation systems for a set of non-overlapping networks: this approach is sometimes used where it is desired to process as many stations as possible (e.g., to contribute to the TRF). This is a parallelization technique as the subnetwork normal equations are generated on separate systems prior to stacking and inversion.
- Double-difference processing: some software packages process double-difference observable combinations to eliminate transmitter and receiver clock offsets from the observations. This reduces the number of parameters at each epoch significantly but still provides access to orbit, EOP, atmospheric delay, and station position parameters. Many science applications of GNSS have no interest in clock offsets and benefit from a reduced computational burden when processing double difference observables.
- Clock densification: high-rate satellite clock parameters required for highly dynamic applications (e.g., kinematic ground stations or kinematic orbit determination of low Earth orbiters, Chap. 32) dramatically increase the number of unknown parameters. For the example network of Table 34.3, more than 500 000 clock parameters would have to be estimated for 30 s sampling. In order to save computation time [34.98] developed a method utilizing epoch-differenced phase observations. This *efficient high-rate clock interpolation (EHRI)* algorithm densifies the 5 min satellite clock parameters obtained from the global clock estimation to 30 s or even 5 s sampling and reduces computation time by a factor of about 10.

34.5 Software

A variety of software packages for GNSS POD have been developed at academic, research, and commercial institutions. We give brief descriptions of some of these below and summarize the products currently produced by each:

- Bernese GNSS Software, developed at the Astronomical Institute of the University of Bern (AIUB). An extensive software package, Bernese is used for GNSS and low Earth orbit (LEO) POD, precise point positioning, estimation of DCBs, antenna calibrations, ionosphere and troposphere estimation, and more. AIUB along with other institutions make up the Center for Orbit Determination in Europe (CODE), which contribute GPS and GLONASS products (orbits, clocks, DCBs, antenna calibrations, troposphere and ionosphere solutions) to the IGS, as well as multi-GNSS products including Galileo, BeiDou, and QZSS to the IGS MGEX [34.68].
- NAPEOS (NAvigation Package for Earth Orbiting Satellites), developed at the European Space Agency (ESA). NAPEOS is used for GNSS and LEO POD, precise point positioning, estimation of DCBs, antenna calibrations, ionosphere and troposphere parameters, etc. NAPEOS is used to generate products at the ESA IGS AC, which contributes GPS and GLONASS POD as well as troposphere and ionosphere products to the IGS [34.99].
- GIPSY (GNSS-Inferred Positioning System and Orbit Analysis Simulation Software) is developed at the National Aeronautics and Space Administration (NASA) Jet Propulsion Laboratory (JPL). GIPSY is used to generate GPS, GLONASS, and LEO orbit and clock products, PPP solutions, ionosphere and troposphere parameters, and produces the JPL AC contributions to the IGS. GIPSY processing supports NASA flight missions (LEOs and aircraft positioning) as well as atmospheric calibrations for the Deep Space Network [34.100], among others.

- EPOS-8 (Earth Parameter and Orbit System), developed at Deutsches GeoForschungsZentrum (GFZ), is another package with broad capabilities for GNSS POD, troposphere/ionosphere estimation, transmitter antenna calibrations, etc. GFZ is an IGS AC providing GPS and GLONASS products, as well as multi-GNSS solutions for Galileo, BeiDou and QZSS to the IGS MGEX [34.101, 102].
- Centre National d'Etudes Spatiales (CNES, French space agency) develops the GINS/DYNAMO software for GNSS POD. It is used by the CNES IGS AC to produce GPS, GLONASS, and Galileo POD solutions on a routine basis. The software is also used for LEO POD processing [34.103].
- The Position and Navigation Data Analysis (PANDA) software developed at Wuhan University, China, is another software package for GNSS and LEO POD. Wuhan University contributes multi-GNSS products to the IGS MGEX project as well as GPS products to the IGS Rapid combination (currently in evaluation mode) [34.104].
- GAMIT-GLOBK is a GPS processing software developed at the Department of Earth Atmospheric and Planetary Sciences at the Massachusetts Institute of Technology(MIT) [34.105], and is used by the MIT IGS AC to contribute weekly final as well as reprocessed products to the IGS.
- PAGES (Program for the Adjustment of GPS EphemerideS) is developed by the U.S. National Geodetic Survey (NGS) [34.106] and is used to produce GPS orbits, station parameters, and EOPs using a double-difference approach. The NGS is an IGS AC contributing ultra-rapid, rapid, final, and reprocessed products.
- A number of commercial services produce precise GNSS POD solutions using both in-house and externally developed software packages. These providers focus primarily on real-time or low-latency postprocessed products of interest to customers operating in areas such as precise marine and land navigation, cellular device positioning, GNSS integrity monitoring, and meteorological analysis. Providers active in this space include John Deere (Navcom) [34.107], JPL Global Differential GNSS System [34.108], Fugro [34.109], RX Networks [34.110], Trimble [34.111], and Veripos [34.112]. These providers in some cases manage their own ground station networks, operate processing centers, provide real-time GNSS orbits and clocks (typically transmitted as corrections to the broadcast ephemeris) and integrity data via geostationary satellite links, and even sell proprietary receiver hardware. GPS and GLONASS products are standard, with BeiDou and Galileo solutions quickly coming online.

34.6 Products

Precise GNSS orbit and clock products must include several items. There are of course the transmitter orbits: these conventionally refer to the CoM and are given as time series of ECEF coordinates and optionally velocities. Given the satellites' altitude, the orbits are sufficiently dynamic to allow accurate interpolation of coordinates given at 15 min intervals (or less) using an 8–11th order interpolator ([34.113] and Annex A.2.1). If desired, the resulting satellite positions can be expressed in an ECI using the EOPs provided along with the orbit and clock products.

Transmitter clock offsets may be provided at various intervals. Solutions submitted to the IGS generally employ intervals of 5 min or 30 s, while intervals as small as 1 s are common in real-time systems. In general, the smaller the interval the better, since a user must interpolate clocks to epochs falling between estimates. Interpolation introduces some error depending on how well the interpolation (typically piecewise-linear) fits the true clock offsets.

It is important to note that clock offsets as provided in the IGS products refer to the transmitter antenna phase center while the orbits refer to the CoM. Since GNSS range data represent the geometric distance between the electrical phase center of the transmitter and receiver antennas, a user must adjust the CoM location given in the orbit product to the phase center. The products should therefore provide information about the phase center model (PCOs and PCVs) used so that a user can apply a consistent model. Metadata, for instance the version of IERS conventions, and the terrestrial reference frame realized in a set of products, is also useful so users can apply consistent models in their processing. This information is provided in the analysis strategy summary files [34.114].

IGS products are commonly named according to latency, including real-time (seconds), ultra-rapid (hours), rapid (next day), final (1–2 weeks), and reprocessed (every few years). Accuracy improves as latency increases for several reasons. Waiting longer tends to increase the available tracking data, especially for outlying stations, improving the distribution of the tracking network. Waiting allows one to use

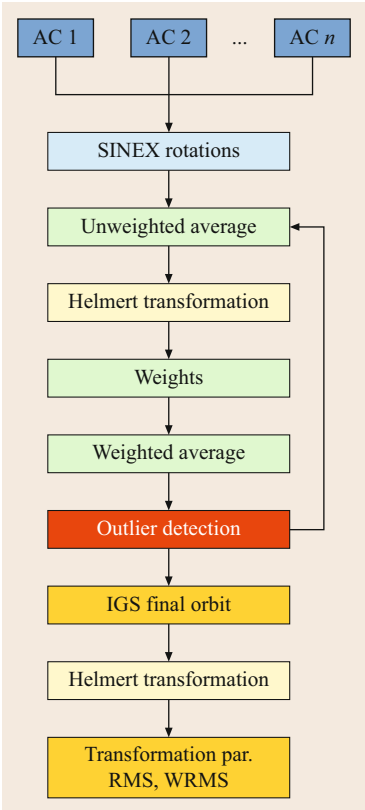

Fig. 34.8 Flow chart of the IGS orbit combination

more accurate nominal orbits and clocks, or provides time to iterate upon solutions to create improved nominals. This particularly benefits the editing of tracking data in preprocessing. One can use raw measurements or linear combinations thereof to detect unreasonable data and carrier-phase cycle slips, but the use of accurate orbit and clocks for data editing greatly enhances ones ability to screen for outlier tracking data. Other nominal models such as EOPs, zenith troposphere and associated mapping functions, and second-order ionosphere also improve as they progress from predicted quantities to estimates based on observations. The chief benefits of reprocessing campaigns are to have all tracking data available and to apply consistent models and estimation strategies over a long time span.

34.6.1 IGS Orbit and Clock Combination

The official IGS orbit and clock products are the result of a combination of the contributions of the individual ACs. Three product lines with different latency and accuracy are provided (Sect. 33.3):

- Ultra-rapid (observed half: 3–9 h, 3 cm, 50 ps)
- Rapid (17–41 h, 2.5 cm, 25 ps)
- Final (12–18 d, 2 cm, 20 ps).

The IGS Analysis Center Coordinator (ACC) is responsible for the generation of the combined products. A combined orbit product provides higher reliability and precision compared to the individual AC orbits. In the following, only the generation of the final orbit and clock products is discussed. The general combination methodology is described in [34.115].

Orbit Combination

Input for the orbit combination are satellite positions provided by the IGS ACs in an ECEF reference frame in SP3 format (Annex A.2.1) at 15 min sampling. The combination is based on an iterative weighted averaging (Fig. 34.8). To guarantee consistency of the station coordinates, EOPs, and orbits, AC-specific rotations are applied to the orbits prior to the actual combination [34.116]. These rotations have previously been derived by the IGS reference frame coordinator based on an analysis and combination of the station coordinates and EOPs that have been delivered by the ACs in the so-called SINEX (Solution Independent Exchange) format

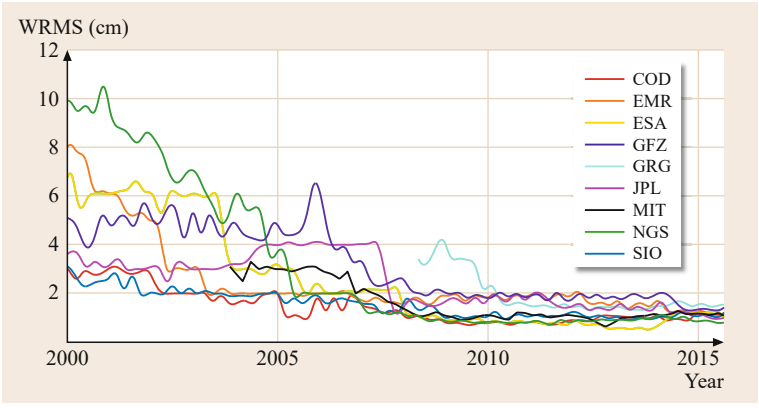

Fig. 34.9 Smoothed WRMS of individual AC GPS orbit solutions w.r.t. combined IGS final orbit

(Annex A.2.3). Detailed statistics as well as information on the combination are given in the weekly IGS combination summary files `igswwww7.sum` (wwww stands for the GPS week), which are available at ftp://ftp.cddis.eosdis.nasa.gov/pub/ in the corresponding wwww subdirectory.

The historical weighted root-mean square (WRMS) of the GPS orbits of the individual ACs w.r.t. the combined IGS final orbit is shown in Fig. 34.9. The comparison of the orbits improves with time due to the application of more sophisticated and consistent models and processing techniques. For example, in August 2007 JPL adopted the igs05.atx antenna model [34.117] already used at the time by the other ACs, resulting in a WRMS decrease by a factor of about 3. Starting with 2008, two groups of ACs can be distinguished: one group agreeing at the 2 cm level (EMR, GRG, JPL, SIO) and another group agreeing at the 1 cm level (COD, ESA, GFZ, MIT, NGS). In April 2014, ESA started to use an a priori box-wing model [34.118]. Although this model improves the orbit quality, it introduces larger differences w.r.t. the other AC solutions [34.119], resulting in a higher WRMS and a lower weight in the combination. As a consequence, the general WRMS of the individual IGS ACs approaches the 1.5 cm level. Further details on the precision of IGS final orbits are given in [34.120]. The combined IGS final GLONASS orbits are generated with the same procedure but in a separate process.

The WRMS of the orbit combination is, however, only a measure of the internal consistency of the orbits, which may suffer from common systematic errors. Harmonics of the draconitic GPS year (time period between the same orientation of the orbital planes w.r.t. the Sun, $\approx$ 351 d for GPS) have been reported for almost all IGS products [34.121]. It was shown that more sophisticated orbit modeling with an adjustable box-wing SRP model can reduce these draconitic errors [34.122]. However, deficiencies in the subdaily EOP model are also identified in [34.121] as causing artificial periodicities around 7, 9, 14, and 29 d due to aliasing.

The optical SLR technique allows for independent validation of the GNSS satellite orbits determined from microwave observations. An SLR analysis of 20 years of GPS and 12 years of GLONASS orbits computed by the CODE AC was performed by [34.123]. They found a 1 cm bias and 2 cm RMS for the two GPS satellites equipped with laser retro-reflectors. Whereas the SLR bias of the GLONASS satellites is in general on the few millimeters level, the RMS is around 3–4 cm. These numbers illustrate the discrepancies between internal precision as represented by the orbit combination WRMS and the accuracy as evaluated by SLR, which are caused by the systematic errors mentioned above.

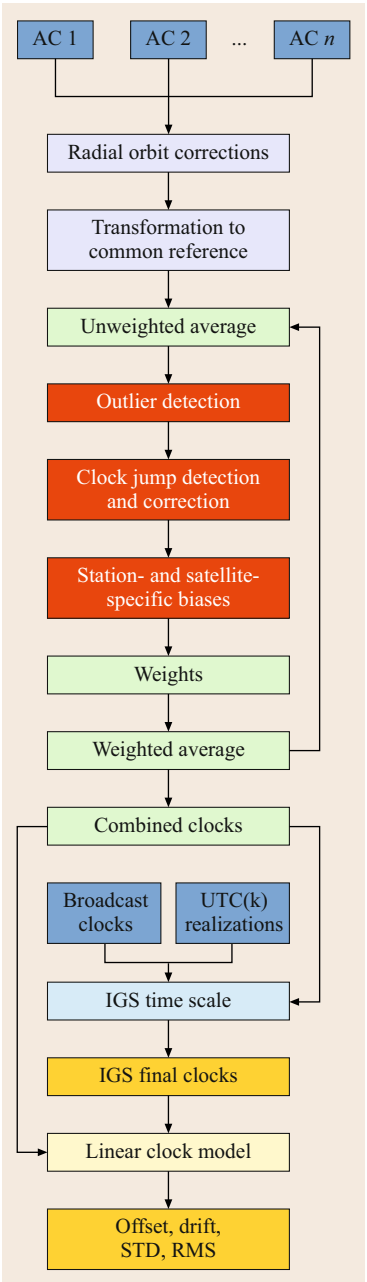

Fig. 34.10 Flow chart of the IGS clock combination. UTC(k) refers to UTC realizations at dedicated timing laboratories with calibrated GPS receivers included in the combined clocks

Clock Combination

Input for the clock combination are satellite and receiver clock estimates in RINEX clock format (Annex A.2.2). The general combination procedure is illustrated in Fig. 34.10 and discussed in more detail in [34.124, 125]. As a first step, radial orbit differences between the combined and individual AC orbits are computed and applied to the clocks in order to remove orbit-related systematic errors (radial or-

bit differences and satellite clock offsets are one-to-one correlated). Then, the individual AC clocks are aligned w.r.t. a common reference. Clock offset and drift w.r.t. a selected reference are removed for all ACs. The reference is taken from either the broadcast clock corrections or the clock estimates of a selected AC aligned to the broadcast clock corrections in a previous step.

During the iterative combination process, outliers are detected and clock jumps are corrected. A weighted average is formed based on weights determined from the deviation of the AC clocks w.r.t. an unweighted mean. The combined clocks are used to realize the IGS timescale (IGST, [34.126]). IGST is aligned to UTC via calibrated GPS receivers at time laboratories (labeled UTC(k) in Fig. 34.10) and GPS time from the navigation message. As a final step, the clock summary files are generated providing offset/drift of a linear clock model and RMS/STD w.r.t. the combined clocks as well as information about the time scale generation.

The historical RMS of the AC-specific GPS clock solutions w.r.t. the combined IGS final clocks is illustrated in Fig. 34.11. SIO does not provide clock corrections and NGS is excluded from the combination as only broadcast clocks are provided (due to double-difference observable processing). The RMS of the most consistent ACs is on the 100 ps level. For GLONASS, no combined clock product is available as mentioned in Sect. 34.4.8.

A critical issue for the clock combination is the consistency of the applied transmitter antenna and attitude models. As an example, all IGS ACs except for JPL switched the antenna model from igs05.atx to igs08.atx in April 2011 [34.127]. For JPL, this switch took place in July 2011 [34.117]. The 3 months of inconsistent antenna modeling can be clearly seen in Fig. 34.11 as JPL's clock RMS increases by a factor of more than 3. Discrepancies among ACs in attitude modeling are evident for the eclipse periods of the GPS Block II/IIA satellites. These cause large clock differences responsible for the rejection of individual ACs during the combination process [34.128]. Figure 34.12 illustrates this problem for GPS Block IIA SVN-33. The MIT clock estimates show a significantly different behavior after the satellite leaves the shadow, resulting in an exclusion of this AC for this particular satellite.

34.6.2 Formats and Transmission

A variety of GNSS product formats and transmission mechanisms are used today (Annex A). Postprocessed products are usually provided as compressed files. Open standards for data exchange include SP3 (standard product 3) for GNSS orbits and clocks [34.129], clock RINEX for receiver and transmitter clocks [34.130], Earth rotation parameter (ERP) [34.131], and antenna exchange (ANTEX) antenna calibration [34.132] formats. Within the IGS, the fourth comment line in the SP3 orbit files is used to document important modeling options including the phase center model, name of the ocean tidal loading and atmospheric tidal loading models, and whether CoM corrections are applied. The full format description of this SP3 comment line is given in [34.133]. Each POD software generally also uses proprietary formats representing the same information, for example, the GIPSY *pos* or Bernese *standard orbit* [34.68] formats.

Real-time systems distribute products via low-latency files (e.g., each minute) as well as few second latency streams. The real-time streams usually represent the precise orbit and clock solution as corrections to the current broadcast navigation message (with respect to a specific issue of data encoded in the corrections message). This implies that the generator of the corrections must account for any differences in the transmitter antenna phase center offsets used to compute the broadcast ephemerides and precise solutions. The user applies the corrections to the broadcast or-

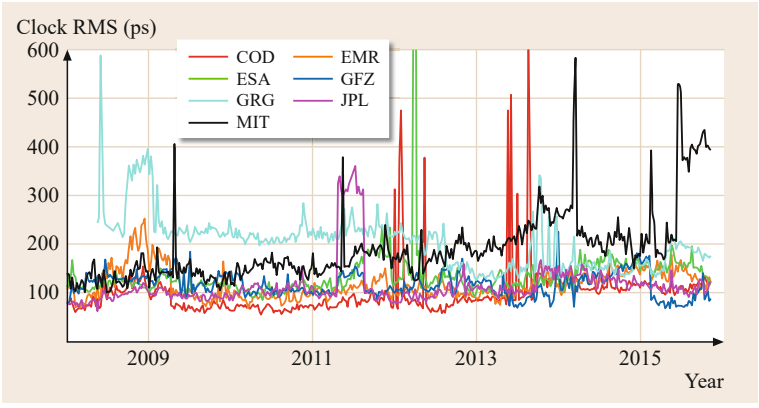

Fig. 34.11 RMS of individual AC clock solutions w.r.t. combined IGS final clocks

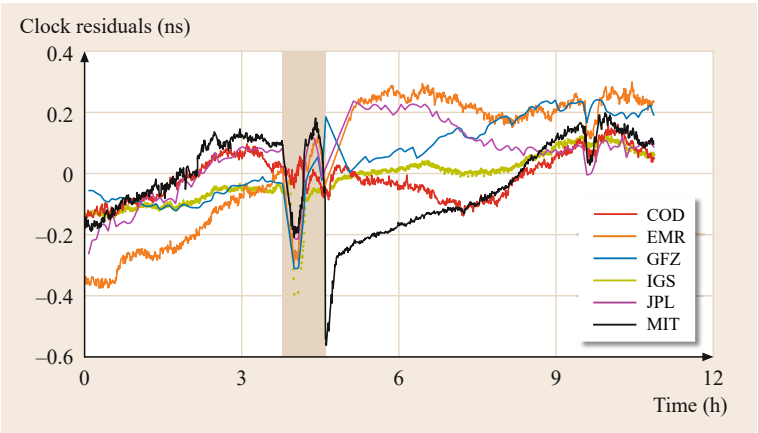

Fig. 34.12 Individual AC and combined IGS clock residuals of the GPS Block IIA satellite SVN-33 for 6 February 2011. The *light brown shaded* area indicates the eclipse period. The ESA clock estimates are used as reference clock and offset/drift of each AC are removed. EMR and MIT clock estimates of this satellite were excluded from the clock combination on that day

bits and clocks directly. The corrections approach has the benefit that some latency (up to tens of seconds) does not significantly degrade the user solution since the navigation message accounts for the majority of the bias and drift in the satellite position and clock, whereas the corrections terms are relatively steady over short time intervals (at least for nominally performing transmitter clocks). Corrections are usually transmitted at 1 s intervals, and losing some corrections over the communication link, or updating at longer intervals, is possible with this approach. Real-time correction streams from commercial providers are encoded in proprietary binary formats sent as TCP or UDP packets over the Internet or transmitted to user equipment via geostationary satellite links [34.134]. The IGS real-time service transmits corrections over the Internet in the open State–Space Representation (SSR) format [34.135].

34.6.3 Using Products

Whether products are acquired as postprocessed files or real-time streams, the user applies a set of precise orbit, clock, and ancillary information in their processing. Maintaining consistency with GNSS products is critical to realizing the best possible accuracy. As discussed, orbits need to be adjusted from the CoM to the antenna phase center, which requires knowledge of both the antenna calibrations and the spacecraft attitude model used to generate the GNSS products. Attitude models in the POD software packages have varying levels of complexity, particularly for non-nominal attitude regimes (e.g., eclipse). The best consistency is therefore achieved by using the same software that generated the products.

The data type to which the clocks products refer should also be consistent. By convention, GPS (broadcast ephemeris and precise) products provide clocks estimated using the L1 P(Y)/L2 P(Y) ionosphere-free linear combination, while GLONASS processing may use either the coarse or precise ranging code to form the ionosphere-free linear combination (it does not matter since the user needs to estimate range biases on each receiver–transmitter link again). For the Galileo and BeiDou CDMA systems conventions are currently developing (Sect. 34.4.8). In any case, the user should process the same data type used to generate the GNSS products. If the data type is not available, the user must apply the appropriate DCBs (e.g., GPS L1 C/A vs. L1 P(Y)) in preprocessing.

34.7 Outlook

For many years the POD community mainly focused on GPS since this was the only stable constellation. Over the course of nearly three decades, the knowledge of physical properties underlying the measurement system have been continually refined. The high accuracies achieved today are enabled by several key factors: taking advantage of tracking data provided by a large, global set of geodetic stations, careful treatment of measurement biases, robust data editing schemes, sophisticated modeling of station motion, atmospheric effects, clock offsets, electrical phase centers, spacecraft dynamics and attitude.

In recent years, the renewal of the GLONASS constellation and the building of Galileo and BeiDou has

resulted in a total of four usable GNSSs. The level of knowledge about the newer systems, and accuracy of POD products, is in many ways comparable to the first decade of precision GPS. The challenges that lie ahead are multifaceted: areas such as the handling of measurement biases between the GNSSs, treatment of more complex signal structures, multi-GNSS ambiguity resolution, and the generation of consistent time scales provide rich grounds for research and development. Details regarding spacecraft attitude control, physical satellite properties and force models, antenna-phase centers, and constellation operations are still in limited distribution. It is, therefore, paramount for the precision GNSS community to engage system operators to make available detailed system information enabling precise POD. For the foreseeable future, GPS will remain the cornerstone of multi-GNSS processing, but the accuracies achieved with the other systems should rapidly improve.

For all GNSSs, model improvements and the determination of clock offsets remain important research topics. Orbit parameters are constrained by well-understood dynamics, but clocks are treated as unconstrained epoch parameters to mitigate for steering, reset events, and other difficult-to-model behaviors. Epoch-independent parameterization, coupled with least-squares estimation, allows clock estimates to absorb model errors to minimize postfit residuals.

Since clock estimates refer to antenna phase centers, accurate models for phase and group delay (receiver and transmitter) and spacecraft attitude are particularly critical. Correlations between receiver clock, geodetic station height, and zenith tropospheric delay are concerns for some science applications. Highly stable satellite clocks may alleviate some of these issues. For instance, the Galileo passive hydrogen masers allow for modeling the clock instead of epoch-wise estimation. It was demonstrated that this approach promises to also improve the orbit quality [34.136].

A challenge for the IGS is the development and implementation of a new software for a fully consistent combination of orbits and clocks of multiple GNSSs, also known as *ACC 2.0*. Currently, combined GPS and GLONASS products are generated by completely separate processing chains. Furthermore, no combined Galileo and BeiDou products are generated although several ACs provide solutions for these systems. The need for such a software upgrade has long been recognized but little progress has been made so far. Related to this, the determination and communication of GNSS timescales in a multi-GNSS world requires an expanded set of signal conventions.

Increasing demands from scientific users drive many of these challenges. GNSS provides important baseline and orientation information to the determination of the global terrestrial reference frame, but does not contribute to geocenter and scale due to the lack of independent, absolute antenna calibrations. Many precise geodetic and atmospheric science applications are taking advantage of the improved spatial and temporal observation coverage offered by multiple GNSS constellations, but continue to observe signals in physical parameters at frequencies related to GNSS spacecraft dynamic forces. The societal benefits provided by emerging low-latency, high-accuracy GNSS applications in areas such as tsunami and earthquake early warning place significant demands on GNSS measurement and processing infrastructure. These are only some examples illustrating the continued promise of precise GNSS POD and its applications, with technical and scientific rewards that will progress well beyond this generation.

Acknowledgments. We would like to thank the Editors for their helpful reviews during the development of this chapter and Mathias Fritsche, Deutsches GeoForschungsZentrum Potsdam (GFZ) for providing information on orbit and clock combination.

References

34.1 O. Montenbruck, P. Steigenberger, A. Hauschild: Broadcast versus precise ephemerides: A multi-GNSS perspective, GPS Solut. **19**(2), 321–333 (2015)

34.2 G. Petit, B. Luzum: *IERS Conventions (2010)*, IERS Technical Note No. 36 (Verlag des Bundesamts für Kartographie und Geodäsie, Frankfurt a. M. 2010)

34.3 M. Rothacher, G. Beutler, T.A. Herring, R. Weber: Estimation of nutation using the Global Positioning System, J. Geophys. Res. **104**(B3), 4835–4859 (1999)

34.4 B.J. Luzum, J.R. Ray, M.S. Carter, F.J. Josties: Recent improvements to IERS Bulletin A combination and prediction, GPS Solut. **4**(3), 34–40 (2001)

34.5 C. Bizouard, D. Gambis: The combined solution C04 for Earth Orientation Parameters consistent with International Terrestrial Reference Frame 2008, Observatoire de Paris, https://hpiers.obspm.fr/iers/eop/eopc04/C04.guide.pdf

34.6 P. Rebischung, J. Griffiths, J. Ray, R. Schmid, X. Collilieux, B. Garayt: IGS08: the IGS realization of ITRF2008, GPS Solut. **16**(4), 483–494 (2012)

34.7 P.M. Mathews, V. Dehant, J.M. Gipson: Tidal station displacements, J. Geophys. Res. **102**(B9), 20469–20477 (1997)

34.8 H.-G. Scherneck: A parametrized solid Earth tide model and ocean loading effects for

global geodetic base-line measurements, Geophys. J. Int. **106**(3), 677–694 (1991)

34.9 F. Lyard, F. Lefevre, T. Letellier, O. Francis: Modelling the global ocean tides: Modern insights from FES2004, Ocean Dyn. **56**(5/6), 394–415 (2006)

34.10 L. Carrere, F. Lyard, A. Guillot, M. Cancet: FES 2012: A new tidal model taking advantage of nearly 20 years of altimetry measurements, Proc. 20 Years Prog. Radar Altimetry Symp., Venice-Lido (CNES/ESA, Toulouse 2012) p. 5

34.11 S.D. Desai: Observing the pole tide with satellite altimetry, J. Geophys. Res. **107**(C11,3180), 1–13 (2003) doi:10.1029/2001JC001224

34.12 R.D. Ray, R.M. Ponte: Barometric tides from ECMWF operational analyses, Ann. Geophys. **21**(8), 1897–1910 (2003)

34.13 J. Boehm, R. Heinkelmann, H. Schuh: Short Note: A global model of pressure and temperature for geodetic applications, J. Geod. **81**(10), 679–683 (2007)

34.14 J. Boehm, A. Niell, P. Tregoning, H. Schuh: Global Mapping Function (GMF): A new empirical mapping function based on numerical weather model data, Geophys. Res. Lett. **33**(L07304), 1–4 (2006) doi:10.1029/2005GL025546

34.15 J. Böhm, G. Möller, M. Schindelegger, G. Pain, R. Weber: Development of an improved empirical model for slant delays in the troposphere (GPT2w), GPS Solut. **19**(3), 433–441 (2014)

34.16 J. Boehm, B. Werl, H. Schuh: Troposphere mapping functions for GPS and very long baseline interferometry from European Centre for Medium-Range Weather Forecasts operational analysis data, J. Geophys. Res. **111**(B02406), 1–9 (2006) doi:10.1029/2005JB003629

34.17 M. Fritsche, R. Dietrich, C. Knöfel, A. Rülke, S. Vey, M. Rothacher, P. Steigenberger: Impact of higher-order ionospheric terms on GPS estimates, Geophys. Res. Lett. **32**(L23311), 1–5 (2005) doi:10.1029/2005GL024342

34.18 N. Ashby: Relativity in the global positioning system, Living Rev. **6**(1), 1–42 (2003) doi:10.12942/lrr-2003-1

34.19 R. Schmid, R. Dach, X. Collilieux, A. Jäggi, M. Schmitz, F. Dilssner: Absolute IGS antenna phase center model igs08.atx: Status and potential improvements, J. Geod. **90**(4), 343–364 (2015)

34.20 J.T. Wu, S.C. Wu, G.G. Hajj, W.I. Bertiger, S.M. Lichten: Effects of antenna orientation on GPS carrier-phase, Manuscr. Geod. **18**, 91–98 (1993)

34.21 O. Montenbruck, R. Schmid, F. Mercier, P. Steigenberger, C. Noll, R. Fatkulin, S. Kogure, A.S. Ganeshan: GNSS satellite geometry and attitude models, Adv. Space Res. **56**(6), 1015–1029 (2015)

34.22 J. Kouba: A simplified yaw-attitude model for eclipsing GPS satellites, GPS Solut. **13**(1), 1–12 (2009)

34.23 F. Dilssner: GPS IIF-1 satellite, antenna phase center and attitude modeling, Inside GNSS **5**(6), 59–64 (2010)

34.24 F. Dilssner, T. Springer, G. Gienger, J. Dow: The GLONASS-M satellite yaw-attitude model, Adv. Space Res. **47**(1), 160–171 (2011)

34.25 X. Dai, M. Ge, Y. Lou, C. Shi, J. Wickert, H. Schuh: Estimating the yaw-attitude of BDS IGSO and MEO satellites, J. Geod. **89**(10), 1005–1018 (2015)

34.26 Y. Ishijima, N. Inaba, A. Matsumoto, K. Terada, H. Yonechi, H. Ebisutani, S. Ukawa, T. Okamoto: Design and development of the first Quasi-Zenith Satellite attitude and orbit control system, IEEE Aerosp. Conf. (2009) doi:10.1109/AERO.2009.4839537

34.27 C.J. Rodriguez-Solano: Impact of Albedo Modelling on GPS Orbits, Master Thesis (TU München, Munich 2009)

34.28 M. Ziebart, S. Edwards, S. Adhya, A. Sibthrope, P. Arrowsmith, P. Cross: High precision GPS IIR orbit prediction using analytical non-conservative force models, Proc. ION GNSS 2004, Long Beach (ION, Virginia 2004) pp. 1764–1770

34.29 IGS: GPS transmit power levels, http://acc.igs.org/orbits/thrust-power.txt

34.30 N.K. Pavlis, S.A. Holmes, S.C. Kenyon, J.K. Factor: The development and evaluation of the Earth Gravitational Model 2008 (EGM2008), J. Geophys. Res. **117**(B04406), 1–38 (2012) doi:10.1029/2011JB008916

34.31 C.C. Finlay, S. Maus, C.D. Beggan, T.N. Bondar, A. Chambodut, T.A. Chernova, A. Chulliat, V.P. Golovkov, B. Hamilton, M. Hamoudi, R. Holme, G. Hulot, W. Kuang, B. Langlais, V. Lesur, F.J. Lowes, H. Luhr, S. Macmillan, M. Mandea, S. McLean, C. Manoj, M. Menvielle, I. Michaelis, N. Olsen, J. Rauberg, M. Rother, T.J. Sabaka, A. Tangborn, L. Toffner-Clausen, E. Thebault, A.W.P. Thomson, I. Wardinski, Z. Wei, T.I. Zvereva: International Geomagnetic Reference Field: The eleventh generation, Geophys. J. Int. **183**(3), 1216–1230 (2010)

34.32 Chalmers University: *Online Ocean Tide Loading Computation Service* http://holt.oso.chalmers.se/loading

34.33 L. Petrov, J.-P. Boy: Study of the atmospheric pressure loading signal in very long baseline interferometry observations, J. Geophys. Res. **109**(B03405), 1–14 (2004) doi:10.1029/2003JB002500

34.34 P. Tregoning, C. Watson, G. Ramillien, H. McQueen, J. Zhang: Detecting hydrologic deformation using GRACE and GPS, Geophys. Res. Lett. **36**(L1540), 1–6 (2009) doi:10.1029/2009GL038718

34.35 P. Misra, P. Enge: *Global Positioning System Signals, Measurements, and Performance*, 2nd edn. (Ganga-Jamuna, Lincoln 2006)

34.36 J. Boehm, H. Schuh: Vienna mapping functions in VLBI analyses, Geophys. Res. Lett. **31**(L01603), 1–4 (2004) doi:10.1029/2003GL018984

34.37 J. Saastamoinen: Atmospheric correction for the troposphere and stratosphere in radio ranging of satellites. In: *The Use of Artificial Satellites for Geodesy*, Geophysical Monograph Series, Vol. 15, ed. by S.W. Henriksen, A. Mancini, B.H. Chovitz

(AGU, Washington 1972) pp. 247–251
34.38 J.L. Davis, T.A. Herring, I.I. Shapiro, A.E.E. Rogers, G. Elgered: Geodesy by radio interferometry: Effects of atmospheric modeling errors on estimates of baseline length, Radio Sci. **20**(6), 1593–1607 (1985)
34.39 D. Bilitza, D. Altadill, Y. Zhang, C. Mertens, V. Truhlik, P. Richards, L. McKinnell, B. Reinisch: The International Reference Ionosphere 2012 – A model of international collaboration, J. Space Weather Space Clim. **4**, A07 (2014)
34.40 S. Kedar, G.A. Hajj, B.D. Wilson, M.B. Heflin: The effect of the second order GPS ionospheric correction on receiver positions, Geophys. Res. Lett. **30**(16), 1–4 (2003) doi:10.1029/2003GL017639
34.41 E.J. Petrie, M. Hernández-Pajares, P. Spalla, P. Moore, M.A. King: A review of higher order ionospheric refraction effects on dual frequency GPS, Surv. Geophys. **32**(3), 197–253 (2011)
34.42 M. Garcia-Fernandez, S.D. Desai, M.D. Butala, A. Komjathy: Evaluation of different approaches to modeling the second-order ionospheric delay on GPS measurements, J. Geophys. Res. Space Phys. **118**(12), 7864–7873 (2013)
34.43 M. Hernández-Pajares, J.M. Juan, J. Sanz, R. Orús: Second-order ionospheric term in GPS: Implementation and impact on geodetic estimates, J. Geophys. Res. **112**(B08417), 1–16 (2007) doi:10.1029/2006JB004707
34.44 S. Bassiri, G.A. Hajj: Higher-order ionospheric effects on the global positioning system observables and means of modeling them, Manuscr. Geod. **18**, 280–289 (1993)
34.45 N. Ashby, J.J. Spilker Jr.: Introduction to relativistic effects on the Global Positioning System. In: *Global Positioning System: Theory and Applications*, Vol. 1, ed. by B.W. Parkinson, J.J. Spilker Jr. (AIAA, Washington 1996) pp. 623–697
34.46 J. Kouba: Relativistic time transformations in GPS, GPS Solut. **5**(4), 1–9 (2002)
34.47 R. Schmid, P. Steigenberger, G. Gendt, M. Ge, M. Rothacher: Generation of a consistent absolute phase center correction model for GPS receiver and satellite antennas, J. Geod. **81**(12), 781–798 (2007)
34.48 Y.E. Bar-Sever: A new model for GPS yaw attitude, J. Geod. **70**(11), 714–723 (1996)
34.49 Y. Bar-Sever, D. Kuang: New empirically derived solar radiation pressure model for Global Positioning System satellites, IPN Prog. Rep. **42**, 159 (2004)
34.50 J.P. Weiss, Y. Bar-Sever, W. Bertiger, S. Desai, M. Garcia-Fernandez, B. Haines, D. Kuang, C. Selle, A. Sibois, A. Sibthorpe: Orbit and attitude modeling at the JPL Analysis Center, Int. GNSS Serv. Workshop, Pasadena (IGS, Pasadena 2014)
34.51 H.F. Fliegel, T.E. Gallini: Solar force modeling of Block IIR Global Positioning System satellites, J. Spacecr. Rockets **33**(6), 863–866 (1996)
34.52 M. Ziebart, S. Adhya, A. Sibthorpe, S. Edwards, P. Cross: Combined radiation pressure and thermal modelling of complex satellites: Algorithms and on-orbit tests, Adv. Space Res. **36**(3), 424–430 (2005)
34.53 P.C. Knocke, J.C. Ries, B.D. Tapley: Earth radiation pressure effects on satellites, Proc. AIAA/AAS Astrodyn. Conf., Minneapolis (AIAA, Reston 1988) pp. 577–587
34.54 M. Ziebart, A. Sibthorpe, P. Cross, Y. Bar-Sever, B. Haines: Cracking the GPS-SLR orbit anomaly, Proc. ION GNSS 2007, Fort Worth (ION, Virginia 2007) pp. 2033–2038
34.55 C.J. Rodriguez-Solano, U. Hugentobler, P. Steigenberger, S. Lutz: Impact of Earth radiation pressure on GPS position estimates, J. Geod. **86**(5), 309–317 (2012)
34.56 B.A. Wielicki, B.R. Barkstrom, E.F. Harrison, R.B. Lee, G.L. Smith, J.E. Cooper: Clouds and the Earth's radiant energy system (CERES): An Earth observing system experiment, Bull. Am. Meteorol. Soc. **77**(5), 853–868 (1996)
34.57 United States Coast Guard: https://www.navcen.uscg.gov/?Do=constellationstatus
34.58 United States Coast Guard: https://www.navcen.uscg.gov/?pageName=currentNanus
34.59 Information and Analysis Center for Positioning, Navigation and Timing: https://www.glonass-iac.ru/en/GLONASS
34.60 Information and Analysis Center for Positioning, Navigation and Timing: https://www.glonass-iac.ru/en/CUSGLONASS/
34.61 European GNSS Service Centre: http://www.gsc-europa.eu/system-status/Constellation-Information
34.62 European GNSS Service Centre: http://www.gsc-europa.eu/system-status/user-notifications
34.63 Cabinet Office: http://qzss.go.jp/en/technical/satellites/index.html#QZSS
34.64 JAXA: http://qz-vision.jaxa.jp/USE/en/naqu
34.65 G.J. Bierman: *Factorization Methods for Discrete Sequential Estimation* (Academic Press, New York 1977)
34.66 P. Axelrad, R.G. Brown: GPS navigation algorithms. In: *Global Positioning System: Theory and Applications*, Vol. 1, ed. by B.W. Parkinson, J.J. Spilker Jr. (AIAA, Washington 1996) pp. 409–433
34.67 B. Tapley, B. Schutz, G.H. Born: *Statistical Orbit Determination* (Academic Press, Burlington 2004)
34.68 R. Dach, F. Andritsch, D. Arnold, S. Bertone, P. Fridez, A. Jäggi, Y. Jean, A. Maier, L. Mervart, U. Meyer, E. Orliac, E. Ortiz-Geist, L. Prange, S. Scaramuzza, S. Schaer, D. Sidorov, A. Sušnik, A. Villiger, P. Walser, C. Baumann, G. Beutler, H. Bock, A. Gäde, S. Lutz, M. Meindl, L. Ostini, K. Sośnica, A. Steinbach, D. Thaller: *Bernese GNSS Software Version 5.2*, ed. by R. Dach, S. Lutz, P. Walser, P. Fridez (Astronomical Institute, University of Bern, Bern 2015)
34.69 M. Rothacher: Estimation of station heights with GPS. In: *Vertical Reference Systems, International Association of Geodesy Symposia*, Vol. 124, ed. by H. Drewes, A.H. Dodson, P.S. Fortes, L. Sanchez, P. Sandoval (Springer, Berlin, Heidelberg 2002)

pp. 81–90
34.70 S. Jin, J. Wang, P.-H. Park: An improvement of GPS height estimations: Stochastic modeling, Earth Planets Space **57**(4), 253–259 (2014)
34.71 X. Luo, M. Mayer, B. Heck, J.L. Awange: A realistic and easy-to-implement weighting model for GPS phase observations, IEEE Trans. Geosci. Remote Sens. **52**(10), 6110–6118 (2014)
34.72 D.S. MacMillan, C. Ma: Atmospheric gradients and the VLBI terrestrial and celestial reference frames, Geophys. Res. Lett. **24**(4), 453–456 (1997)
34.73 O. Titov, V. Tesmer, J. Boehm: OCCAM v. 6.0 software for VLBI data analysis, Proc. IVS 2004 Gen. Meet. (2004) pp. 267–271
34.74 S. Wu, T.P. Yunck, C.L. Thornton: Reduced-dynamic technique for precise orbit determination of low Earth satellites, J. Guid. Control Dyn. **14**(1), 24–30 (1991)
34.75 G. Beutler, E. Brockmann, W. Gurtner, U. Hugentobler, L. Mervart, M. Rothacher, A. Verdun: Extended orbit modeling techniques at the CODE processing center of the international GPS service for geodynamics (IGS): Theory and initial results, Manuscr. Geod. **19**, 367–386 (1994)
34.76 T.A. Springer, G. Beutler, M. Rothacher: A new solar radiation pressure model for GPS satellites, GPS Solut. **2**(3), 50–62 (1999)
34.77 D. Arnold, M. Meindl, G. Beutler, R. Dach, S. Schaer, S. Lutz, L. Prange, K. Sośnica, L. Mervart, A. Jäggi: CODE's new solar radiation pressure model for GNSS orbit determination, J. Geod. **89**(8), 775–791 (2015)
34.78 A. Sibthorpe, W. Bertiger, S.D. Desai, B. Haines, N. Harvey, J.P. Weiss: An evaluation of solar radiation pressure strategies for the GPS constellation, J. Geod. **85**(8), 505–517 (2011)
34.79 N. Romero: CC2NONCC update to handle more than 24 satellites per epoch, IGSMAIL-6542 (2012) https://igscb.jpl.nasa.gov/pipermail/igsmail/2012/007732.html
34.80 P. Steigenberger, O. Montenbruck, U. Hessels: Performance evaluation of the early CNAV navigation message, Navigation **62**(3), 219–228 (2015)
34.81 O. Montenbruck, A. Hauschild, P. Steigenberger: Differential code bias estimation using multi-GNSS observations and global ionosphere maps, Navigation **61**(3), 191–201 (2014)
34.82 L. Mervart: Ambiguity Resolution Techniques in Geodetic and Geodynamic Applications of the Global Positioning System, Ph.D. Thesis, Geodätisch-geophysikalische Arbeiten in der Schweiz, Vol. 53 (Schweizerische Geodätische Kommission, Zürich 1995)
34.83 M. Ge, G. Gendt, G. Dick, F.P. Zhang: Improving carrier-phase ambiguity resolution in global GPS network solutions, J. Geod. **79**(1), 103–110 (2005)
34.84 S. Loyer, F. Perosanz, F. Mercier, H. Capdeville, J.-C. Marty: Zero-difference GPS ambiguity resolution at CNES–CLS IGS Analysis Center, J. Geod. **86**(11), 991–1003 (2012)
34.85 P. Steigenberger, U. Hugentobler, S. Loyer, F. Perosanz, L. Prange, R. Dach, M. Uhlemann, G. Gendt, O. Montenbruck: Galileo orbit and clock quality of the IGS multi-GNSS experiment, Adv. Space Res. **55**(1), 269–281 (2015)
34.86 O. Montenbruck, P. Steigenberger, U. Hugentobler: Enhanced solar radiation pressure modeling for Galileo satellites, J. Geod. **89**(3), 283–297 (2015)
34.87 P. Steigenberger, U. Hugentobler, A. Hauschild, O. Montenbruck: Orbit and clock analysis of Compass GEO and IGSO satellites, J. Geod. **87**(6), 515–525 (2013)
34.88 J. Liu, D. Gua, B. Ju, Z. Shen, Y. Lai, D. Yi: A new empirical solar radiation pressure model for BeiDou GEO satellites, Adv. Space Res. **57**(1), 234–244 (2016)
34.89 Russian Institute of Space Device Engineering: Global Navigation Satellite System GLONASS – Interface Control Document, v5.1, (Russian Institute of Space Device Engineering, Moscow 2008)
34.90 L. Wanninger: Carrier-phase inter-frequency biases of GLONASS receivers, J. Geod. **86**(2), 139–148 (2012)
34.91 International GNSS Service Analysis Center Coordinator, http://acc.igs.org/
34.92 Z. Deng, Q. Zhao, T. Springer, L. Prange, M. Uhlemann: Orbit and clock determination – BeiDou, Proc. IGS Workshop, Pasadena (IGS, Pasadena 2014)
34.93 P. Rebischung: IGb08, IGSMAIL-6663 (2012) https://igscb.jpl.nasa.gov/pipermail/igsmail/2012/006655.html
34.94 X. Wu, J. Ray, T. van Dam: Geocenter motion and its geodetic and geophysical implications, J. Geodyn. **58**, 44–66 (2012)
34.95 R. Ferland, G. Gendt, T. Schöne: IGS reference frame maintenance, Celebrating a decade of the International GPS Service, Workshop and Symposium 2004, Bern, ed. by M. Meindl (Astronomical Institute, University of Bern, Bern 2005) pp. 13–34
34.96 CODE Analysis Strategy Summary (2016) https://igscb.jpl.nasa.gov/igscb/center/analysis/code.acn
34.97 A. Hauschild, O. Montenbruck: Real-time clock estimation for precise orbit determination of LEO-satellites, Proc. ION GNSS 2008, Savannah (ION, Virginia 2008) pp. 581–589
34.98 H. Bock, R. Dach, A. Jäggi, G. Beutler: High-rate GPS clock corrections from CODE: Support of 1 Hz applications, J. Geod. **83**(11), 1083–1094 (2009)
34.99 T.A. Springer: *NAPEOS Mathematical Models and Algorithms*, DOPS-SYS-TN-0100-OPS-GN (ESA/ESOC, Darmstadt 2009)
34.100 JPL: GIPSY-OASIS, https://gipsy-oasis.jpl.nasa.gov
34.101 G. Gendt, G. Dick, W. Soehne: GFZ analysis center of IGS – Annual report 1998. In: *IGS 1998 Technical Reports*, ed. by K. Goway, R. Neilan, A. Moore (JPL, Pasadena 1998) pp. 79–87
34.102 M. Ge, G. Gendt, G. Dick, F.P. Zhang, M. Rothacher: A new data processing strategy for huge GNSS global networks, J. Geod. **80**(4), 199–203 (2006)
34.103 J.C. Marty, S. Loyer, F. Perosanz, F. Mercier, G. Bracher, B. Legresy, L. Portier, H. Capdeville, F. Fund, J.M. Lemoine: GINS: The CNES/GRGS GNSS

scientific software, Proc. 3rd Int. Coll. Sci. Fundam. Asp. Galileo Program., ESA WPP326, Copenhagen (ESA, Noordwijk 2011)
34.104 Q. Zhao, J. Guo, M. Li, L. Qu, Z. Hu, C. Shi, J. Liu: Initial results of precise orbit and clock determination for COMPASS navigation satellite system, J. Geod. **87**(5), 475–486 (2013)
34.105 MIT: GAMIT-GLOBK, http://www-gpsg.mit.edu/~simon/gtgk/
34.106 W.G. Kass, R.L. Dulaney, J. Griffiths, S. Hilla, J. Ray, J. Rohde: Global GPS data analysis at the National Geodetic Survey, J. Geod. **83**(3/4), 289–295 (2009)
34.107 K. Dixon: StarFire: A global SBAS for sub-decimeter precise point positioning, Proc. ION GNSS 2006, Fort Worth (ION, Virginia 2006) pp. 2286–2296
34.108 Global Differential GNSS System, http://www.gdgps.net
34.109 J. Tegedor, D. Lapucha, O. Ørpen, E. Vigen, T. Melgard, R. Strandli: The new G4 service: Multi-constellation precise point positioning including GPS, GLONASS, Galileo and BeiDou, Proc. ION GNSS+ 2015, Tampa (ION, Virginia 2015) pp. 1089–1095
34.110 E. Derbez, R. Lee: GPStream: A low bandwidth architecture to deliver or autonomously generate predicted ephemeris, Proc. ION GNSS 2008, Savannah (ION, Virginia 2008) pp. 1258–1264
34.111 M. Glocker, H. Landau, R. Leandro, M. Nitschke: Global precise multi-GNSS positioning with Trimble Centerpoint RTX, Proc. 6th ESA Workshop Satell. Navig. Technol. Eur. Workshop GNSS Signals Signal Proces. (NAVITEC), Noordwijk (IEEE, New York 2012), doi:10.1109/NAVITEC.2012.6423060
34.112 C. Rocken, L. Mervart, J. Johnson, Z. Lukes, T. Springer, T. Iwabuchi, S. Cummins: A new real-time global GPS and GLONASS precise positioning correction service: Apex, Proc. ION GNSS 2011, Portland (ION, Virginia 2011) pp. 1825–1838
34.113 Y. Feng, Y. Zheng: Efficient interpolations to GPS orbits for precise wide area applications, GPS Solut. **9**(4), 273–282 (2005)
34.114 IGS Analysis Strategy Summaries (2016) ftp://igs.org/pub/center/analysis
34.115 G. Beutler, J. Kouba, T. Springer: Combining the orbits of the IGS analysis centers, Bull. Geod. **69**, 200–222 (1995)
34.116 J. Griffiths: Misalignment of the AC final orbits (2012) http://acc.igs.org/orbits/acc_report_final_rotations.pdf
34.117 S. Desai, W. Bertiger, B. Haines, D. Kuang, C. Selle, A. Sibois, A. Sibthorpe, J. Weiss: JPL IGS analysis center report, 2005–2012, Int. GNSS Serv. Techn. Rep. 2011, Pasadena, ed. by M. Meindl, R. Dach, Y. Jean (IGS Central Bureau, Pasadena 2012) pp. 85–90
34.118 C. Garcia Serrano, L. Agrotis, F. Dilssner, J. Feltens, M. van Kints, I. Romero, T. Springer, W. Enderle: The ESA/ESOC analysis center progress and improvements, IGS Workshop 2014, Pasadena (IGS Central Bureau, Pasadena 2014)
34.119 T. Springer, M. Otten, C. Flohrer, F. Pereira, F. Gini, W. Enderle: GNSS satellite orbit modeling at ESOC, IGS Workshop 2014, Pasadena (IGS Central Bureau, Pasadena 2014)
34.120 J. Griffiths, J. Ray: On the precision and accuracy of IGS orbits, J. Geod. **83**(3/4), 277–287 (2009)
34.121 J. Griffiths, J.R. Ray: Sub-daily alias and draconitic errors in the IGS orbits, GPS Solut. **17**(3), 413–422 (2012)
34.122 C.J. Rodriguez-Solano, U. Hugentobler, P. Steigenberger, M. Bloßfeld, M. Fritsche: Reducing the draconitic errors in GNSS geodetic products, J. Geod. **88**(6), 559–574 (2014)
34.123 K. Sośnica, D. Thaller, R. Dach, P. Steigenberger, G. Beutler, D. Arnold, A. Jäggi: Satellite laser ranging to GPS and GLONASS, J. Geod. **89**(7), 725–743 (2015)
34.124 J. Kouba, T. Springer: New IGS station and satellite clock combination, GPS Solut. **4**(4), 31–36 (2001)
34.125 F.J. Gonzalez Martinez: Performance of New GNSS Satellite Clocks, Ph.D. Thesis (Karlsruher Institut für Technologie, Karlsruhe 2014)
34.126 K. Senior: Report of the IGS working group on clock products, 19th Meet. Consult. Comm. Time Freq., Sèvres (BIPM, Sèvres 2012) pp. 219–236
34.127 J. Ray: REMINDER: Switch to IGS08/igs08.atx on 17 April 2011 IGSMAIL-6384 (2011) https://igscb.jpl.nasa.gov/pipermail/igsmail/2011/007574.html
34.128 J.R. Ray, J. Griffiths: Status of IGS orbit modeling and areas for improvement, Geophys. Res. Abstr. **13** (EGU, Vienna 2011) EGU2011-3774
34.129 S. Hilla: The Extended Standard Product 3 Orbit Format (SP3-c) (2010) https://igscb.jpl.nasa.gov/igscb/data/format/sp3c.txt
34.130 J. Ray, W. Gurtner: RINEX Extensions to Handle Clock Information (2006) https://igscb.jpl.nasa.gov/igscb/data/format/rinex_clock300.txt
34.131 J. Kouba, Y. Mireault: New IGS ERP Format (version 2), IGSMAIL-1943 (1998) https://igscb.jpl.nasa.gov/mail/igsmail/1998/msg00170.html
34.132 M. Rothacher and R. Schmid: ANTEX: The Antenna Exchange Format, Version 1.4 (2010) https://igscb.jpl.nasa.gov/igscb/station/general/antex14.txt
34.133 G. Gendt: IGS switch to absolute antenna model and ITRF2005, IGSMAIL-5438 (2006) https://igscb.jpl.nasa.gov/pipermail/igsmail/2006/005509.html
34.134 G. Maral, M. Bousquet: *Satellite Communications Systems: Systems, Techniques, and Technology*, 5th edn. (Wiley, Chichester 2009)
34.135 Radio Technical Commission for Maritime Services (RTCM): Differential GNSS (Global Navigation Satellite Systems) Services – Version 3 (2013)
34.136 S. Hackel, P. Steigenberger, U. Hugentobler, M. Uhlemann, O. Montenbruck: Galileo orbit determination using combined GNSS and SLR observations, GPS Solut. **19**(1), 15–25 (2015)